Gaia DPAC

INAF

ISTITUTO NAZIONALE DI ASTROFISICA
OSSERVATORIO ASTROFISICO DI TORINO

agenzia spaziale italiana

Testing gravity with Gaia

Mariateresa Crosta

INAF
Osservatorio Astrofisico di Torino

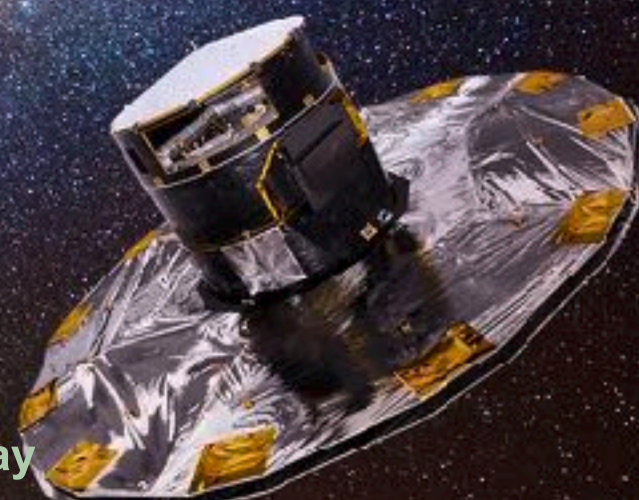

Vulcano Workshop 2018, 21-26 May

Gaia

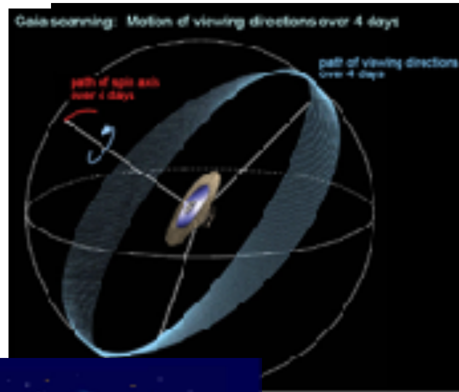
Gaia scanning: Motion of viewing directions over 4 days
path of viewing directions over 4 days
path of spin axis over 4 days

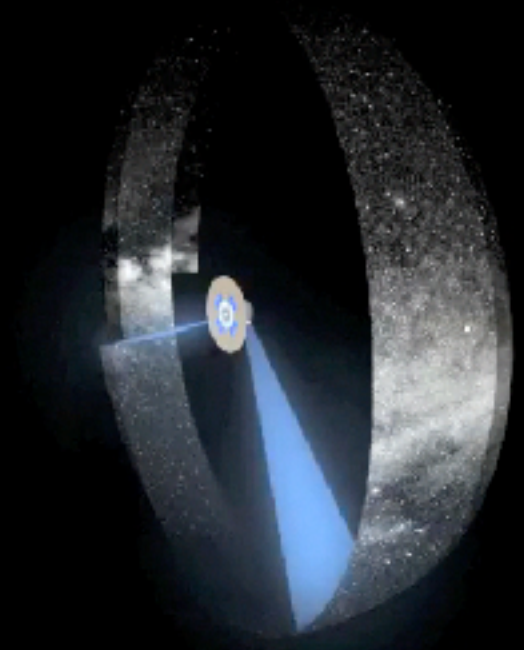


Gaia launch and orbit
(Credit: EADS Astrium)
5 - 6 years of (almost) continuous observation
Lissajous orbit around L2
~1 orbit correction per month
~1 month transfer orbit to L2
Soyuz/Fregat launch from Kourou (French Guyana)
Earth-Moon barycentre, a = 1 AU

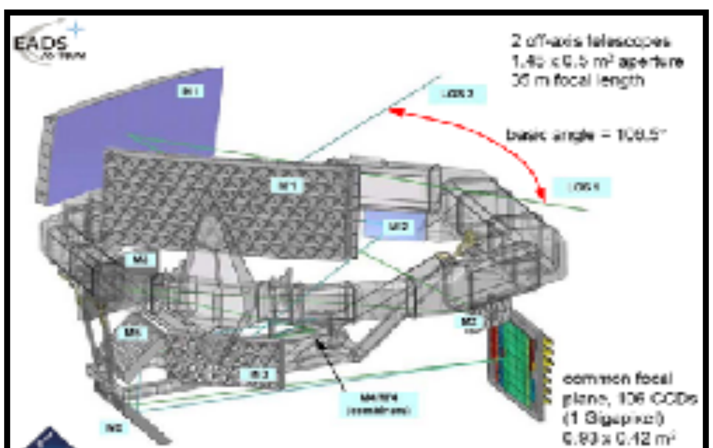
EADS
2 off-axis telescopes
1.45 x 0.5 m² aperture
35 m focal length
basic angle = 106.5°
common focal plane, 106 CCDs
(1 Gigapixel)
0.93 x 0.42 m²

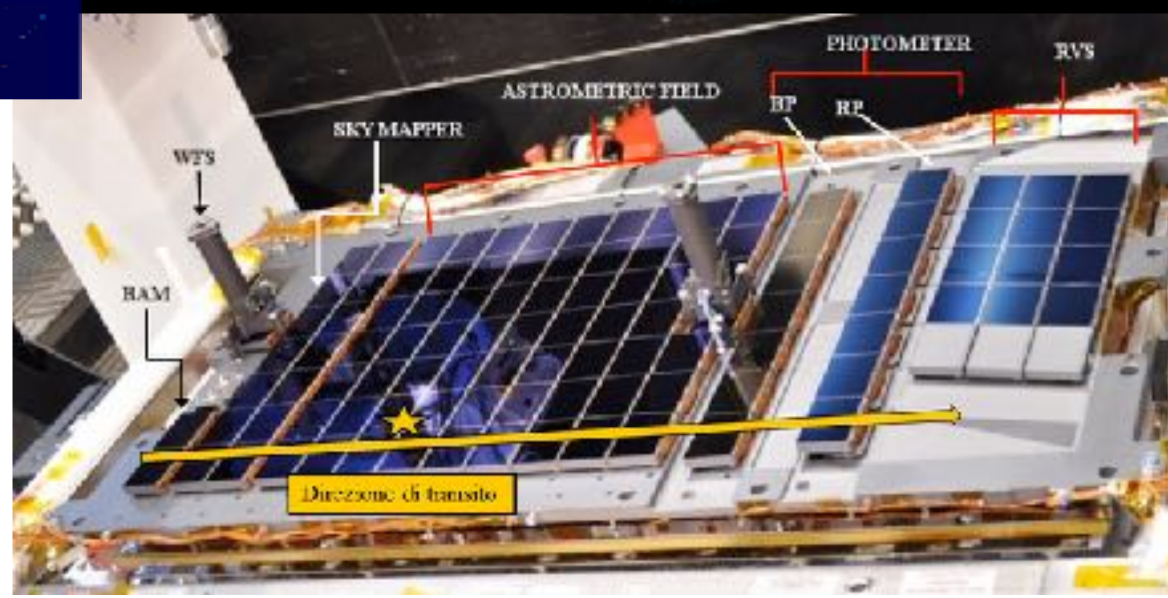
PHOTOMETER
RVS
ASTROMETRIC FIELD
BP
RP
SKY MAPPER
WFS
BAM
Direzione di transito

Gaia

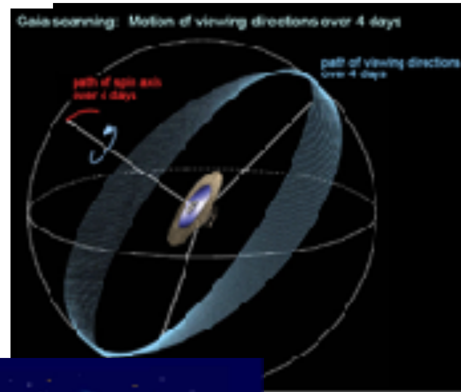
Gaia scanning: Motion of viewing directions over 4 days
path of viewing directions over 4 days

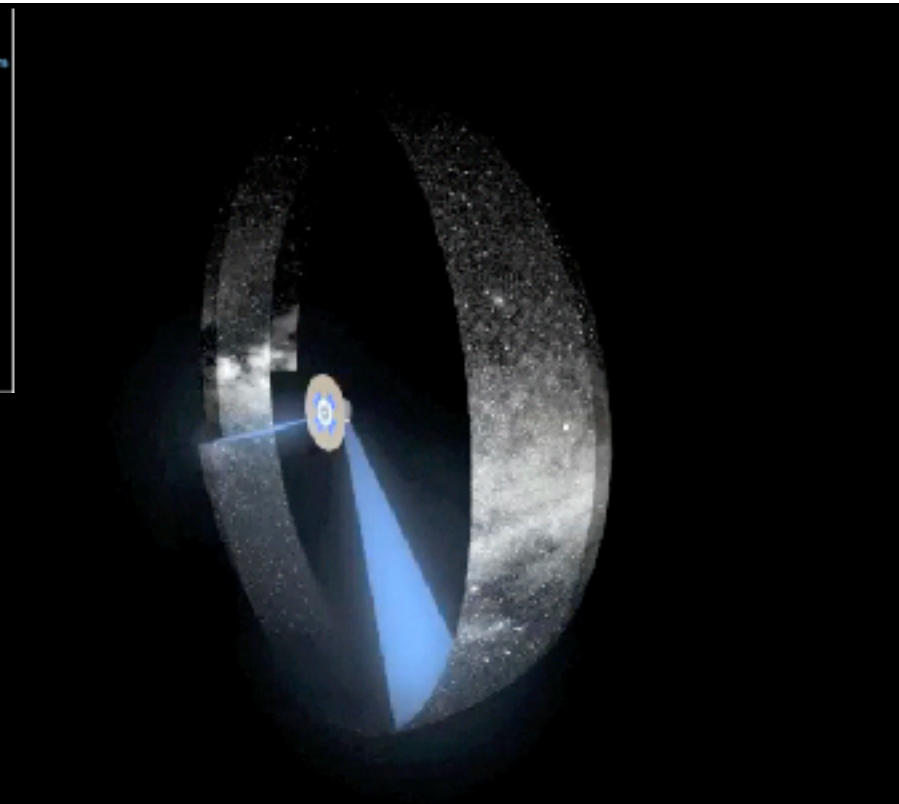


Gaia launch and orbit
(Credit: EADS Astrium)
5 - 6 years of (almost) continuous observation
Lissajous orbit around L_2 ~1 orbit correction per month
~1 month transfer orbit to L_2
L_2 at a = 1.01 AU
Soyuz/Fregat launch from Kourou (French Guyana)
Earth-Moon barycentre, a = 1 AU

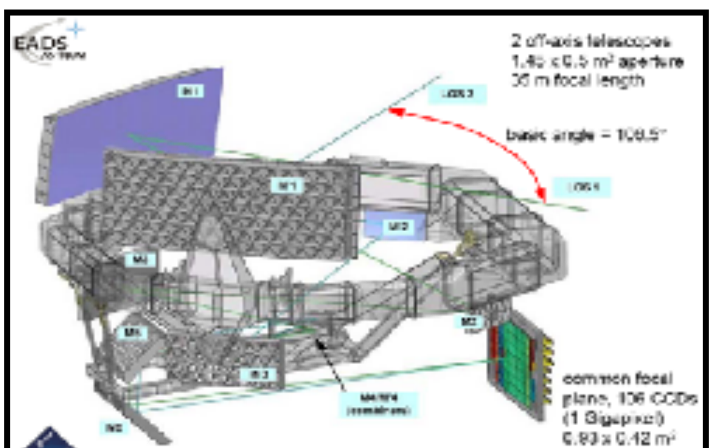
EADS
2 off-axis telescopes
1.45 x 0.5 m² aperture
35 m focal length
basic angle = 106.5°
common focal plane, 106 CCDs (1 Gigapixel) 0.93 x 0.42 m²

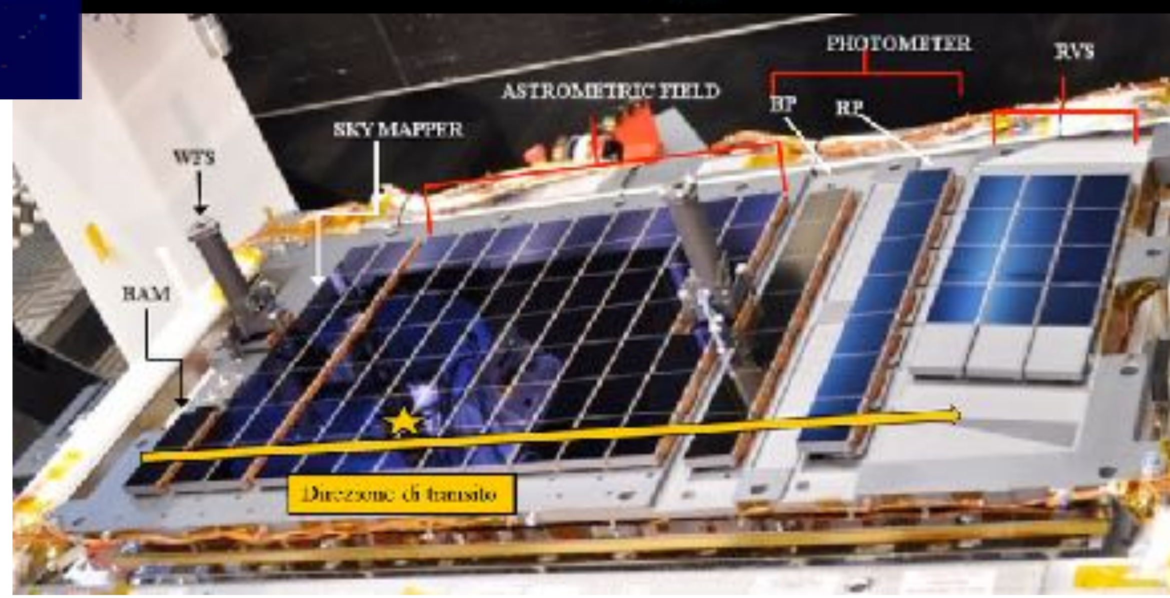
PHOTOMETER
RVS
ASTROMETRIC FIELD
BP
RP
SKY MAPPER
WFS
BAM
Direzione di transito

Gaia – main characteristics and status

https://www.cosmos.esa.int/web/gaia/home

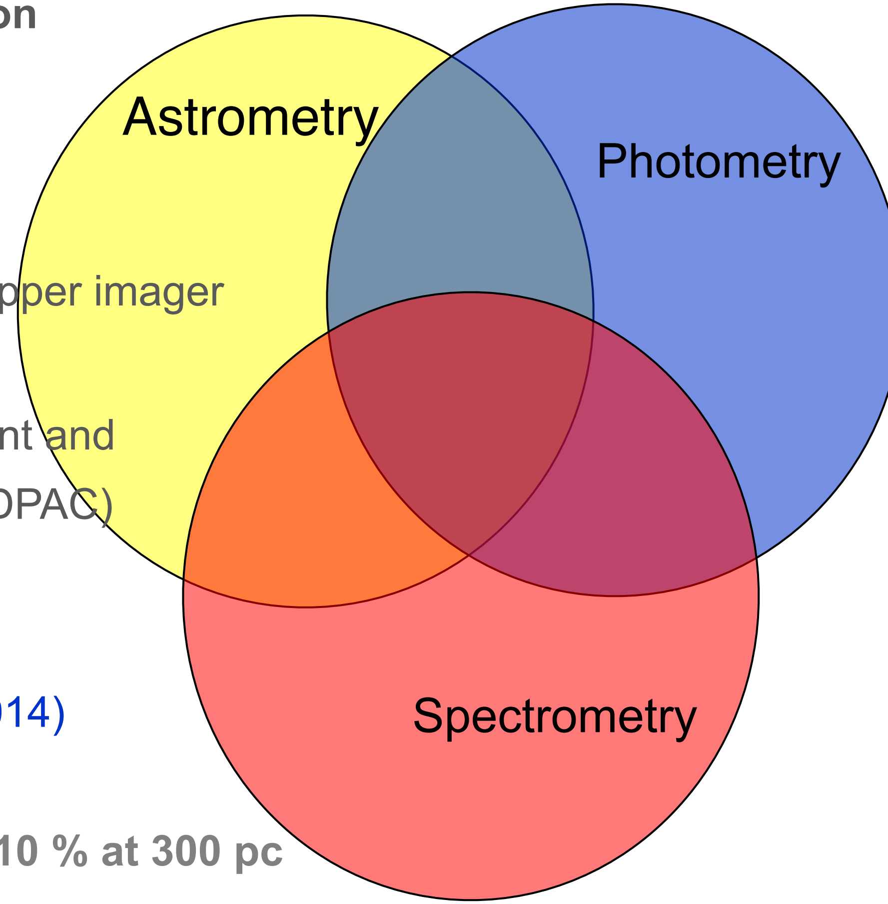

science with **one/two billion objects in 3 dimension**

from structure and evolution of the MW to GR

Astrometry, photometry, spectroscopy (RVS)

- Astrometry and photometry G < 20.7 mag
- Stars brighter than G=3 captured with Sky Mapper imager
- Spectra still to G_{RVS}=16.2

Satellite (including payload) by industry, management and operations by ESA, data processing by scientists (DPAC)

Nominal mission end: mid-2019

Extension: possible up to end-of-2023 ± 1 year

✓ Now in 5-year routine operations (since 25/7/2014)

✓ First DR end of summer 2016

2 million stars complete to V=11.5, sub-mas: 10 % at 300 pc

✓ Second DR on April 25th 2018, 22 months of data collection

1.3 billion stars complete astrometry (parallax) between G=12 and G=17, 100 muas: 10 % 1kpc, solar neighborhood much more detailed

✓ Last DR in 2022 (or 2025) with full accuracy (10 µas for the bright stars)

Data Release Scenario http://www.cosmos.esa.int/web/gaia/release

Gaia – main characteristics and status

https://www.cosmos.esa.int/web/gaia/home

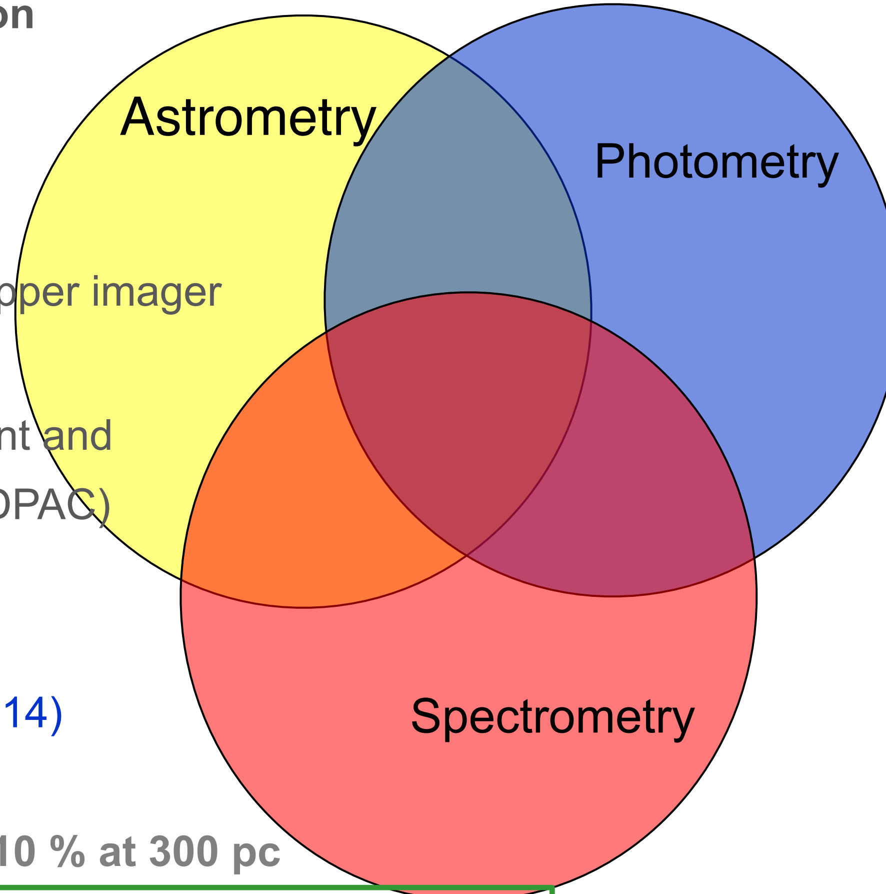

science with **one/two billion objects in 3 dimension**

<u>from structure and evolution of the MW to GR</u>

Astrometry, photometry, spectroscopy (RVS)

- Astrometry and photometry G < 20.7 mag
- Stars brighter than G=3 captured with Sky Mapper imager
- Spectra still to G_{RVS}=16.2

Satellite (including payload) by industry, management and operations by ESA, data processing by scientists (DPAC)

Nominal mission end: mid-2019

Extension: possible up to end-of-2023 ± 1 year

✓ Now in 5-year routine operations (since 25/7/2014)

✓ First DR end of summer 2016

2 million stars complete to V=11.5, sub-mas: 10 % at 300 pc

✓ Second DR on April 25th 2018, 22 months of data collection

1.3 billion stars complete astrometry (parallax) between G=12 and G=17, 100 muas: 10 % 1kpc, solar neighborhood much more detailed

✓ Last DR in 2022 (or 2025) with full accuracy (10 µas for the bright stars)

Data Release Scenario http://www.cosmos.esa.int/web/gaia/release

Second Data Release Scenario
https://www.cosmos.esa.int/web/gaia/dr2

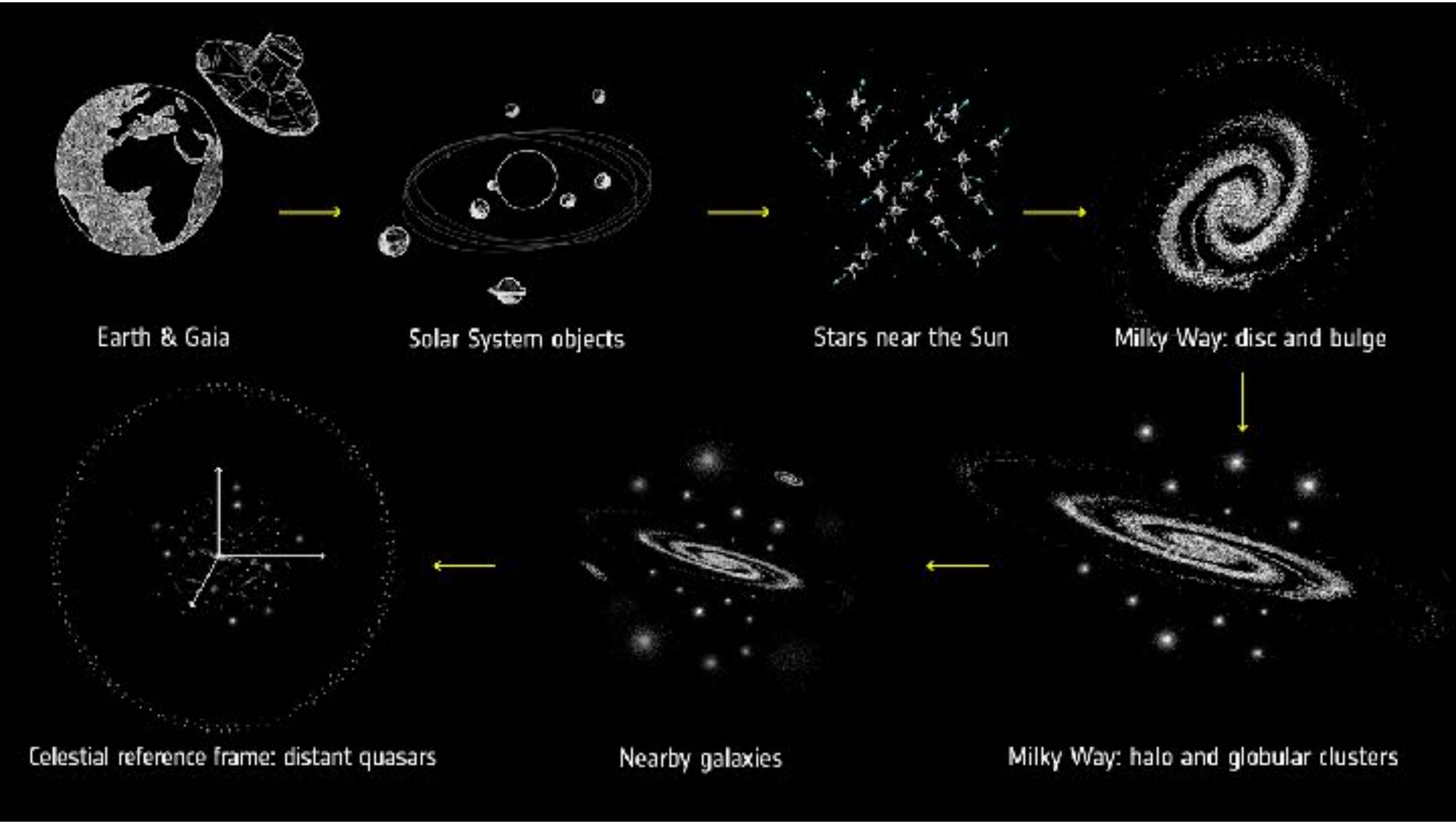

Second Data Release Scenario
https://www.cosmos.esa.int/web/gaia/dr2

Gaia's look into the Milky Way

http://www.cosmos.esa.int/web/gaia/science

Gaia's look into the Milky Way

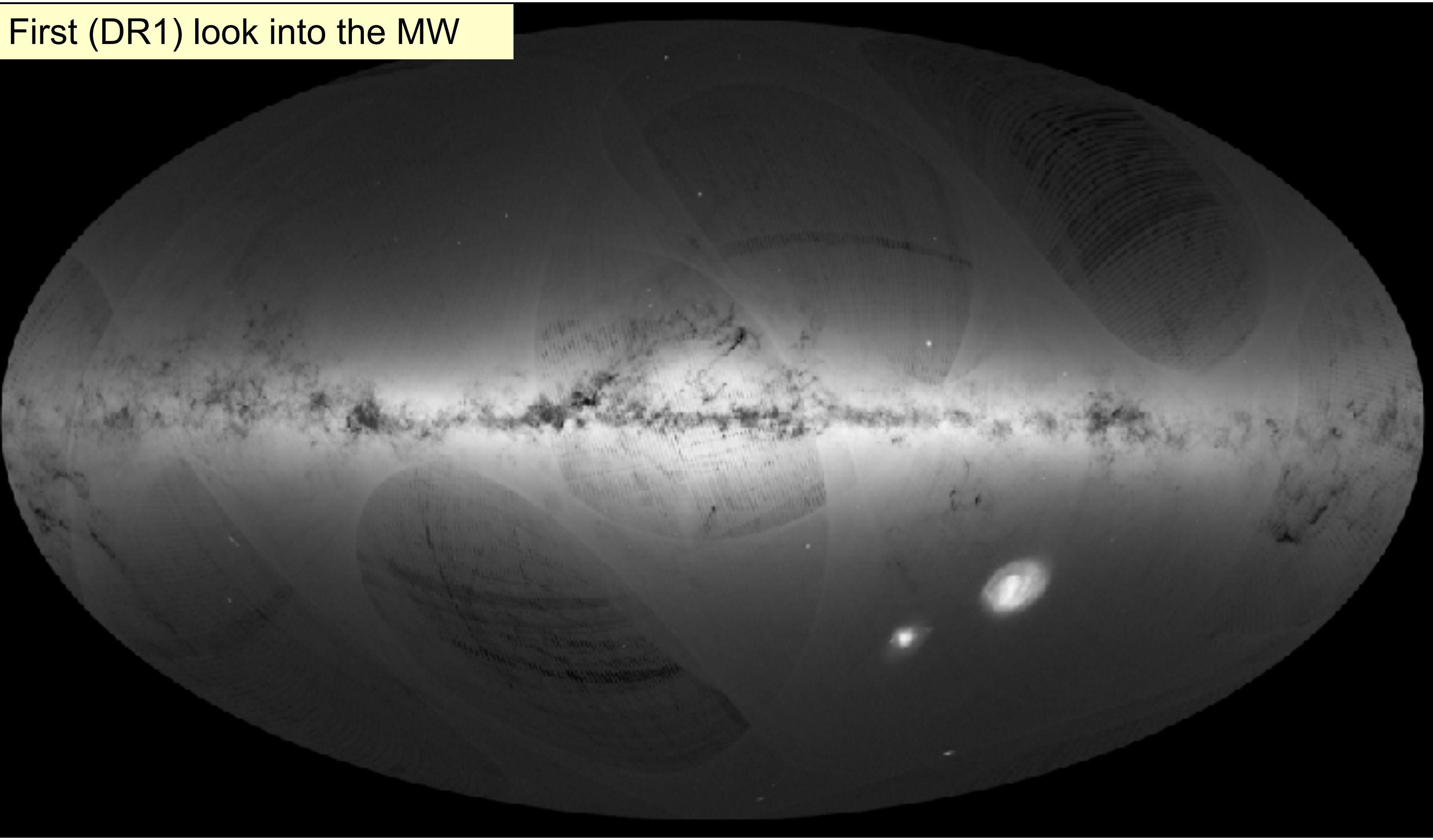

http://www.cosmos.esa.int/web/gaia/science

Gaia’s look into the Milky Way

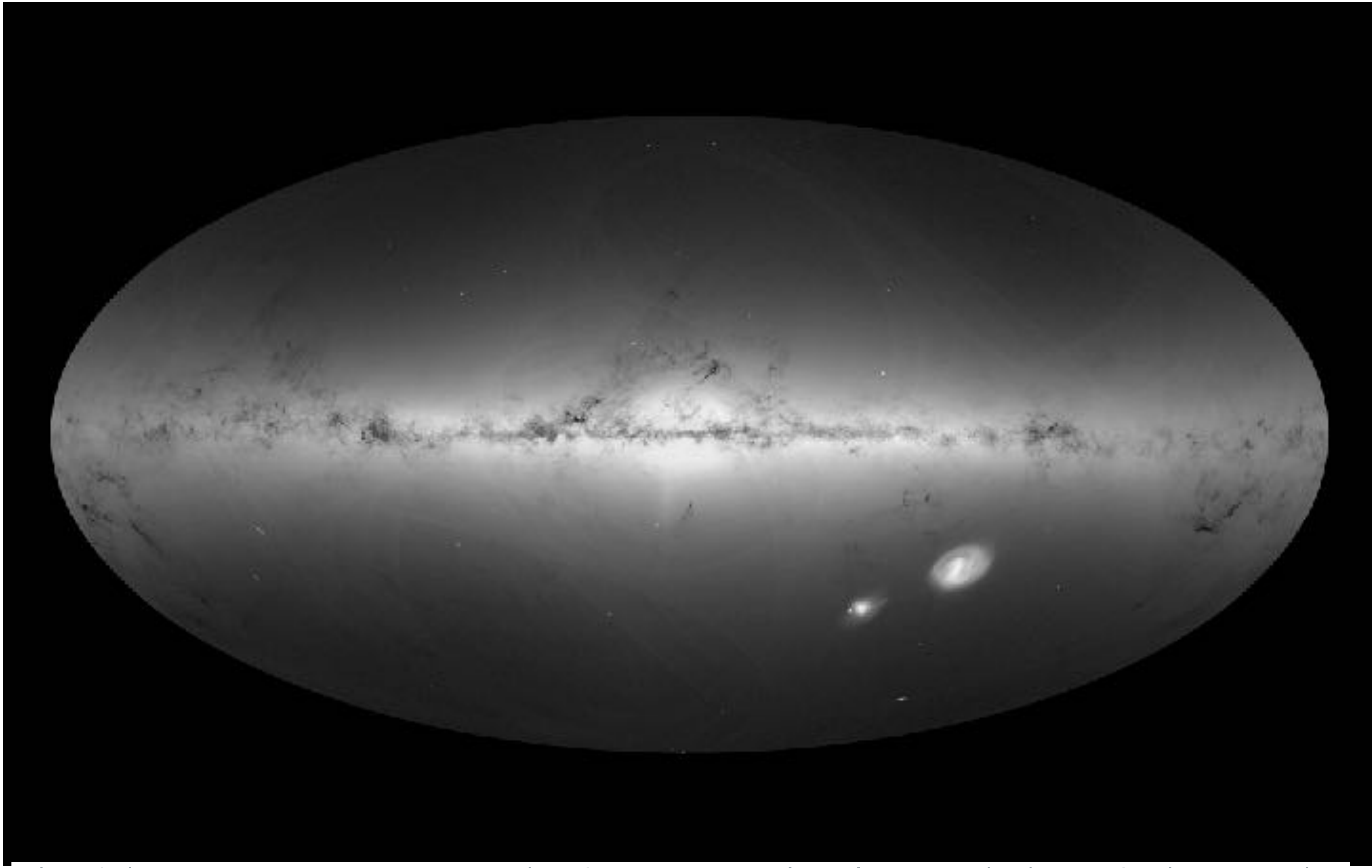

Acknowledgement: Gaia Data Processing and Analysis Consortium (DPAC); A. Moitinho / A. F. Silva / M. Barros / C. Barata, University of Lisbon, Portugal; H. Savietto, Fork Research, Portugal.

Gaia's look into the Milky Way

Second (DR2) look into the MW

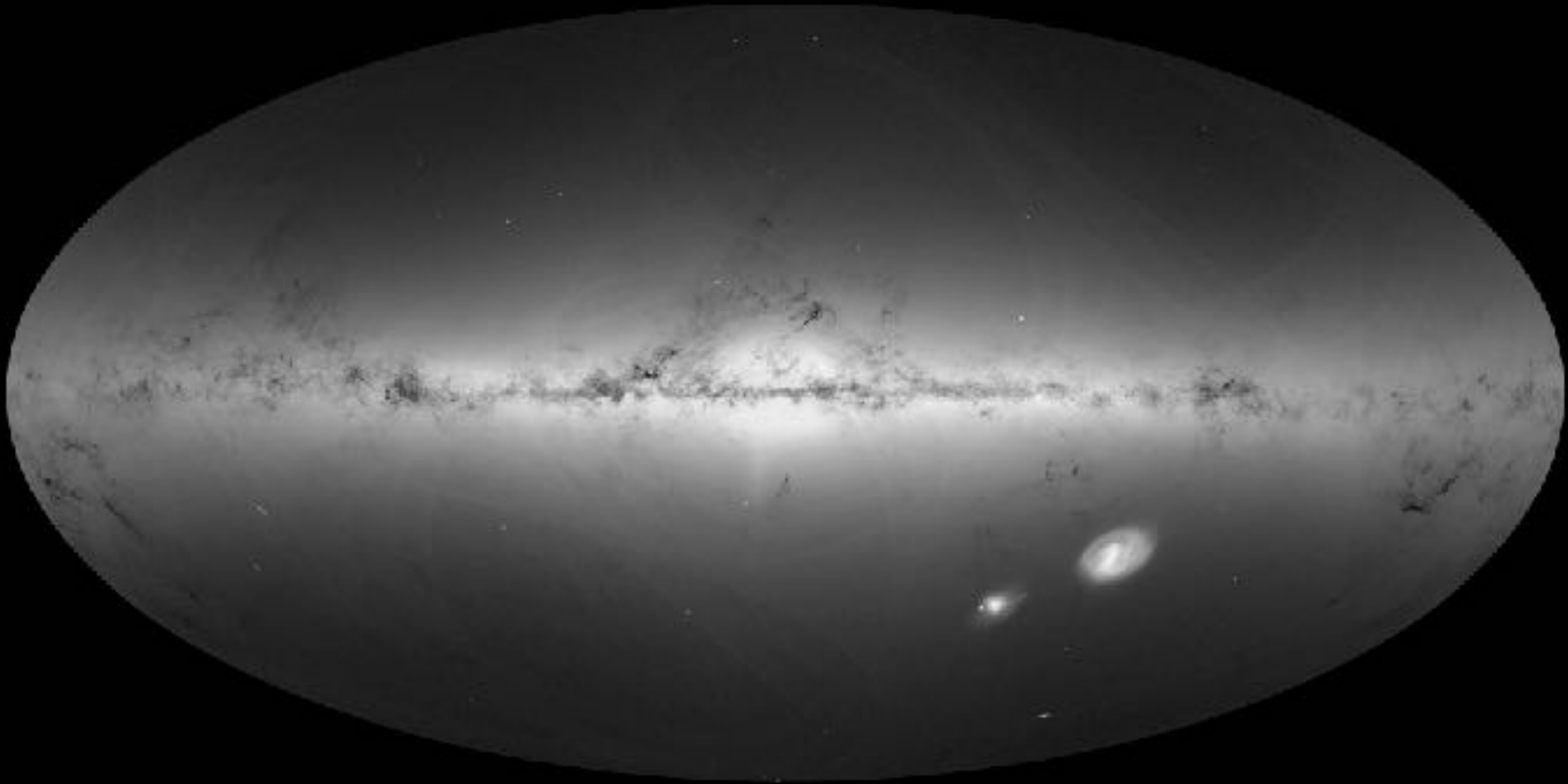

Acknowledgement: Gaia Data Processing and Analysis Consortium (DPAC); A. Moitinho / A. F. Silva / M. Barros / C. Barata, University of Lisbon, Portugal; H. Savietto, Fork Research, Portugal.

Gaia's look into the Milky Way

Second (DR2) look into the MW

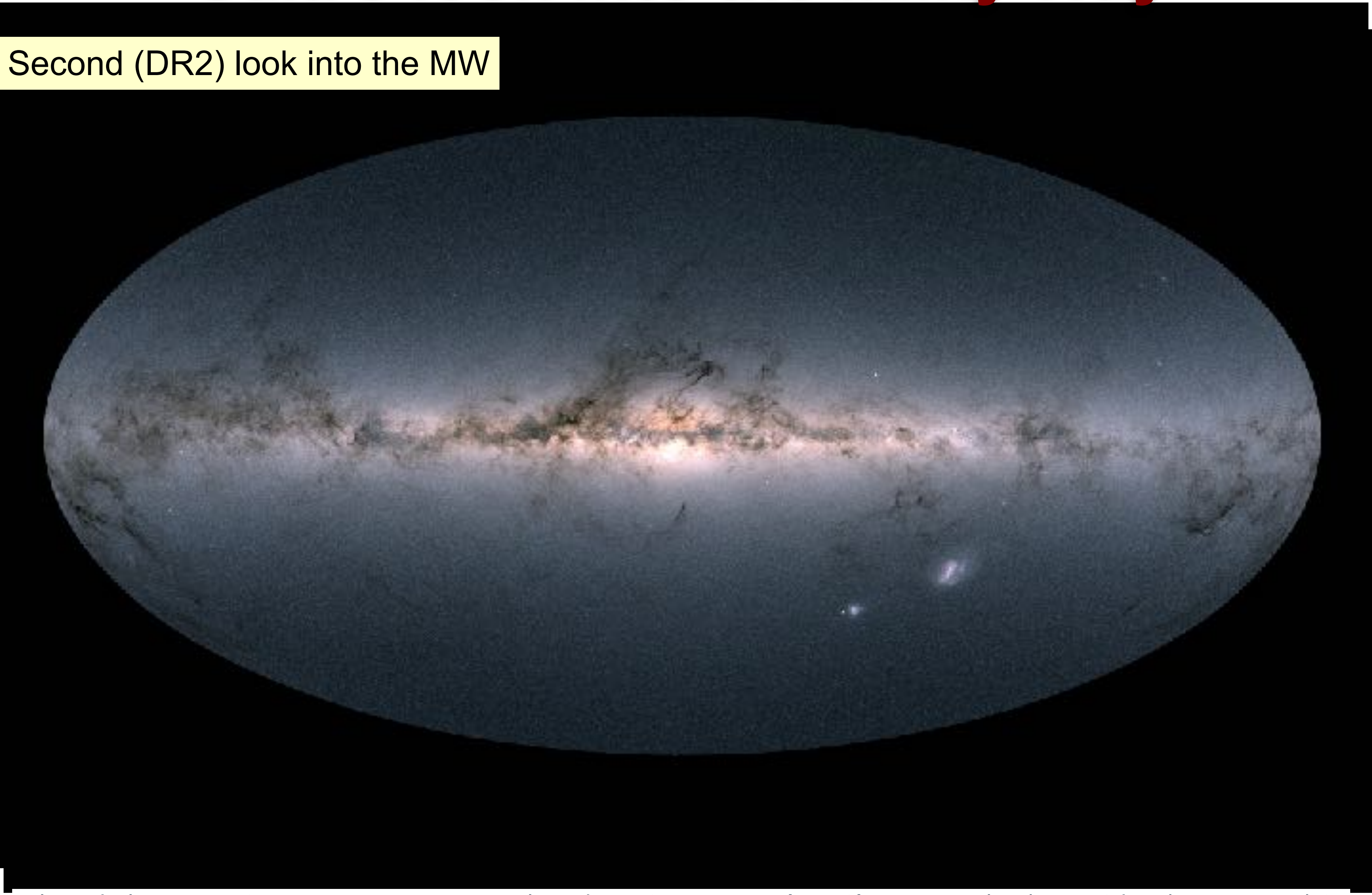

Acknowledgement: Gaia Data Processing and Analysis Consortium (DPAC); A. Moitinho / A. F. Silva / M. Barros / C. Barata, University of Lisbon, Portugal; H. Savietto, Fork Research, Portugal.

Gaia's look into the Milky Way

Second (DR2) look into the MW

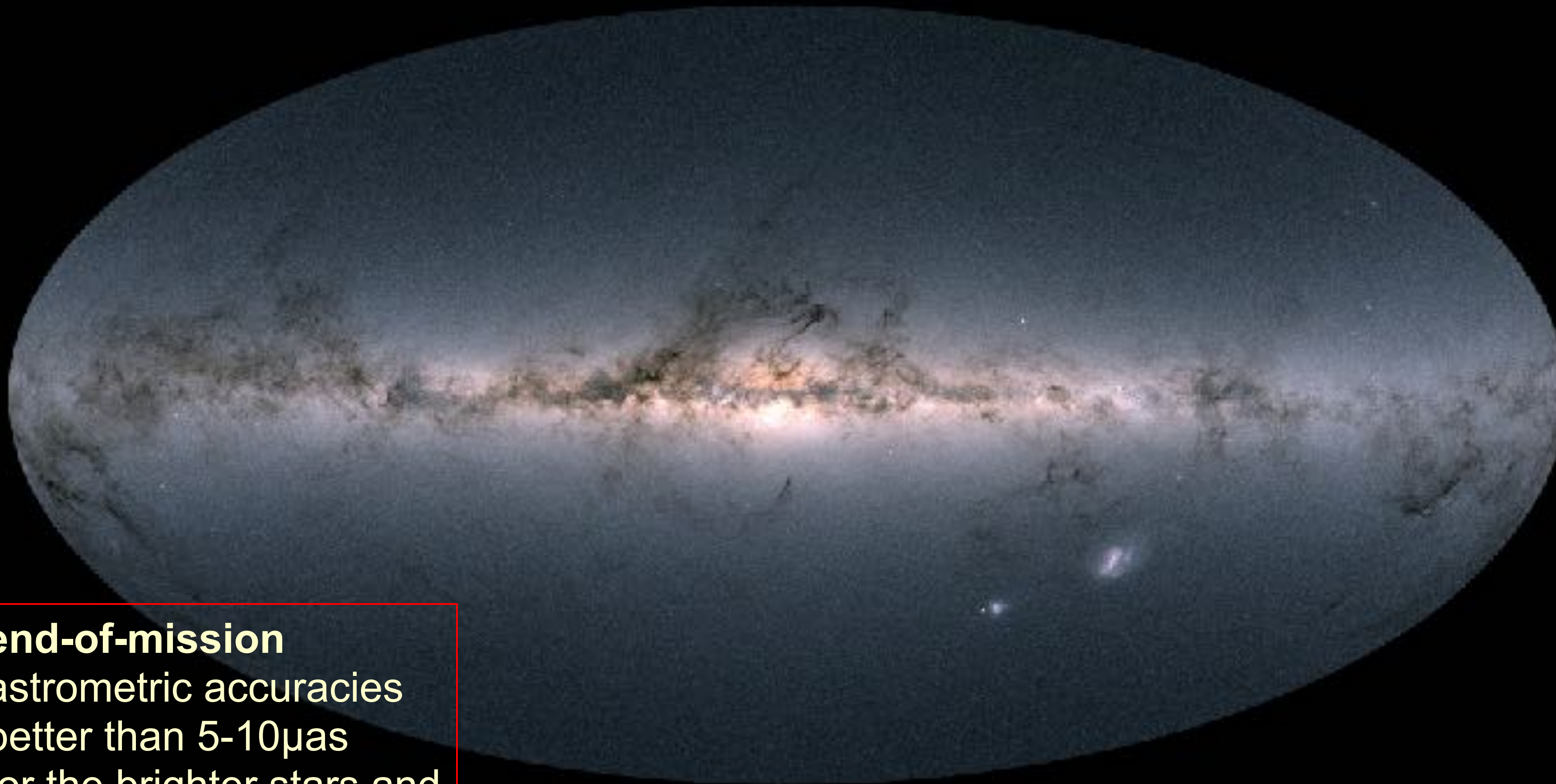

end-of-mission
astrometric accuracies better than 5-10μas for the brighter stars and 130-600μas for faint targets

Acknowledgement: Gaia Data Processing and Analysis Consortium (DPAC); A. Moitinho / A. F. Silva / M. Barros / C. Barata, University of Lisbon, Portugal; H. Savietto, Fork Research, Portugal.

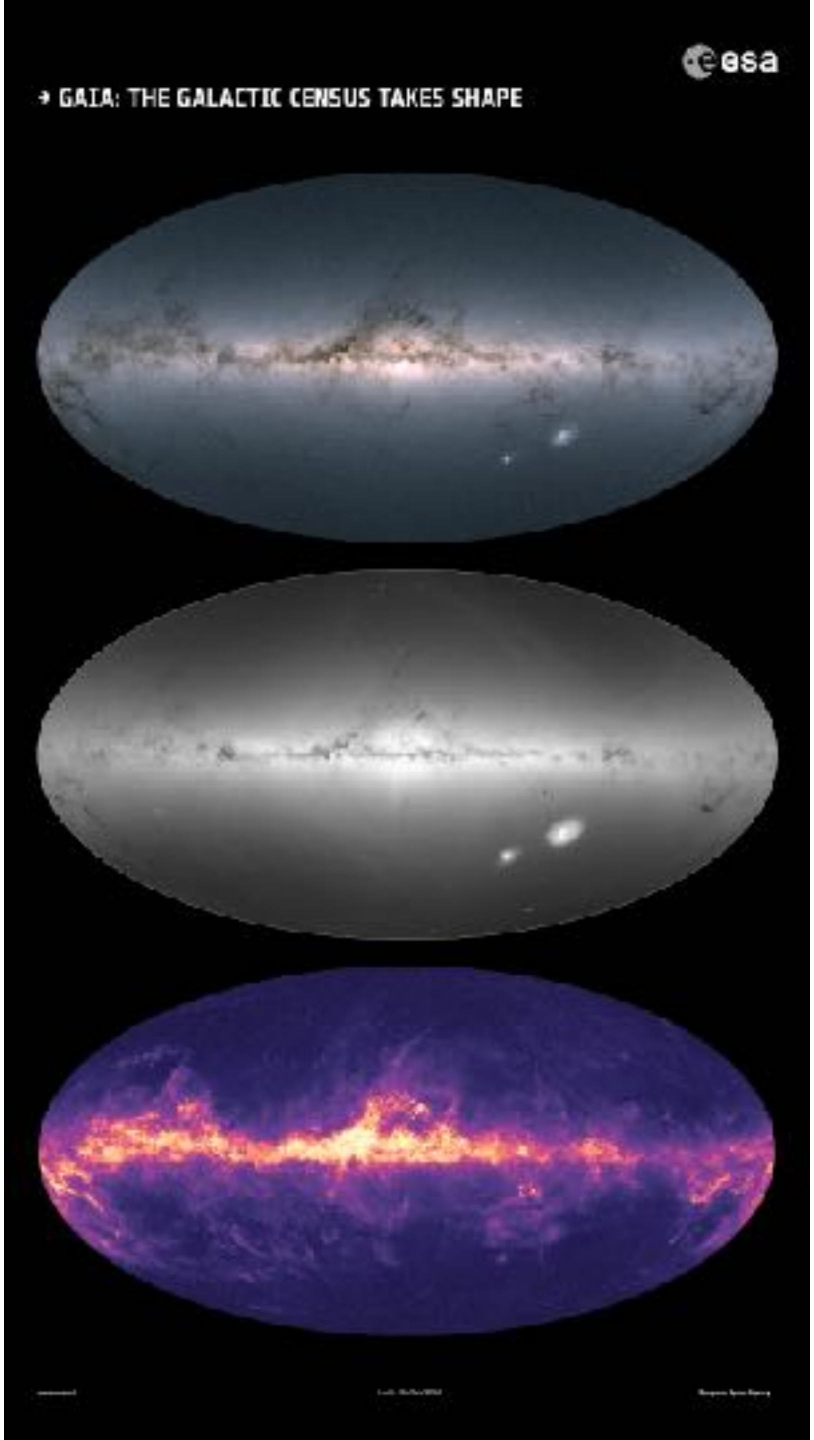

GAIA'S HERTZSPRUNG-RUSSELL DIAGRAM

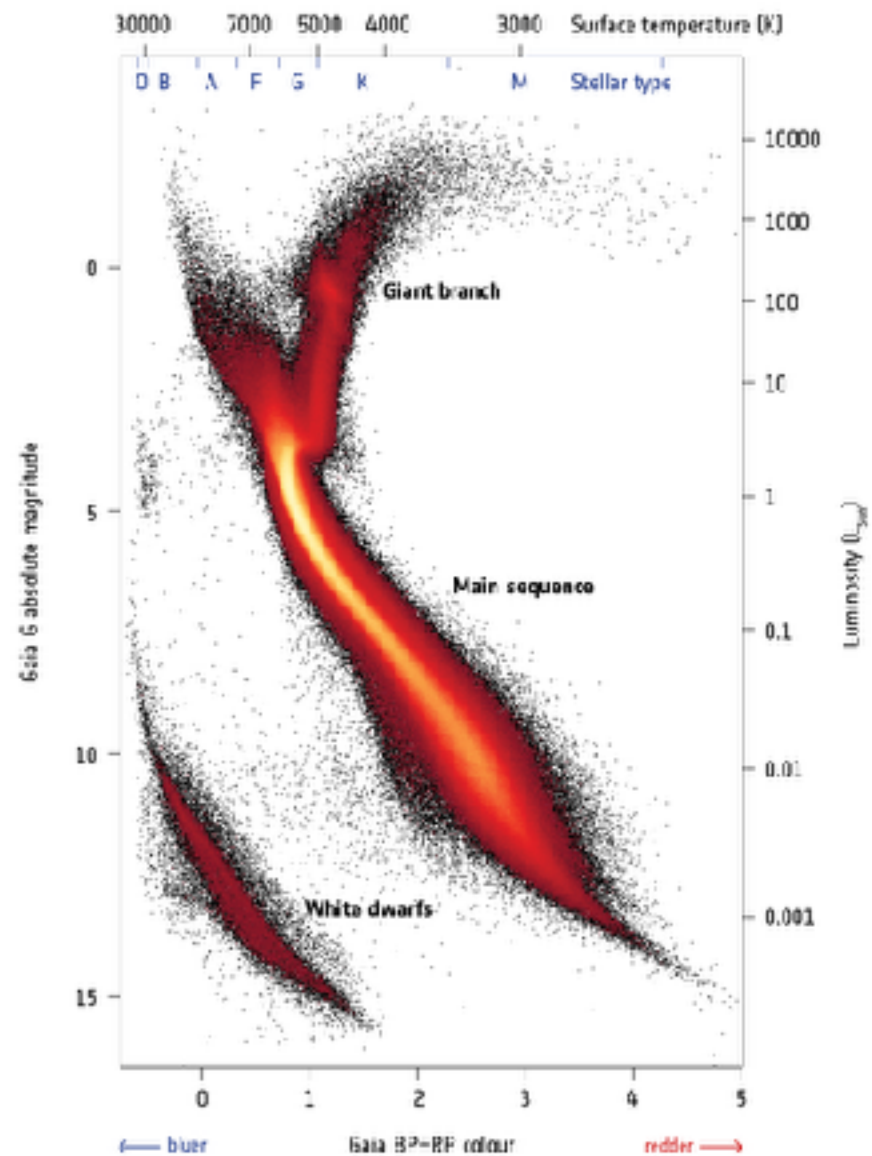

Our laboratory: the Solar System

micro-arcsecond accuracy+ dynamical gravitational fields=> relativistic models of light propagation:
RELATIVISTIC ASTROMETRY

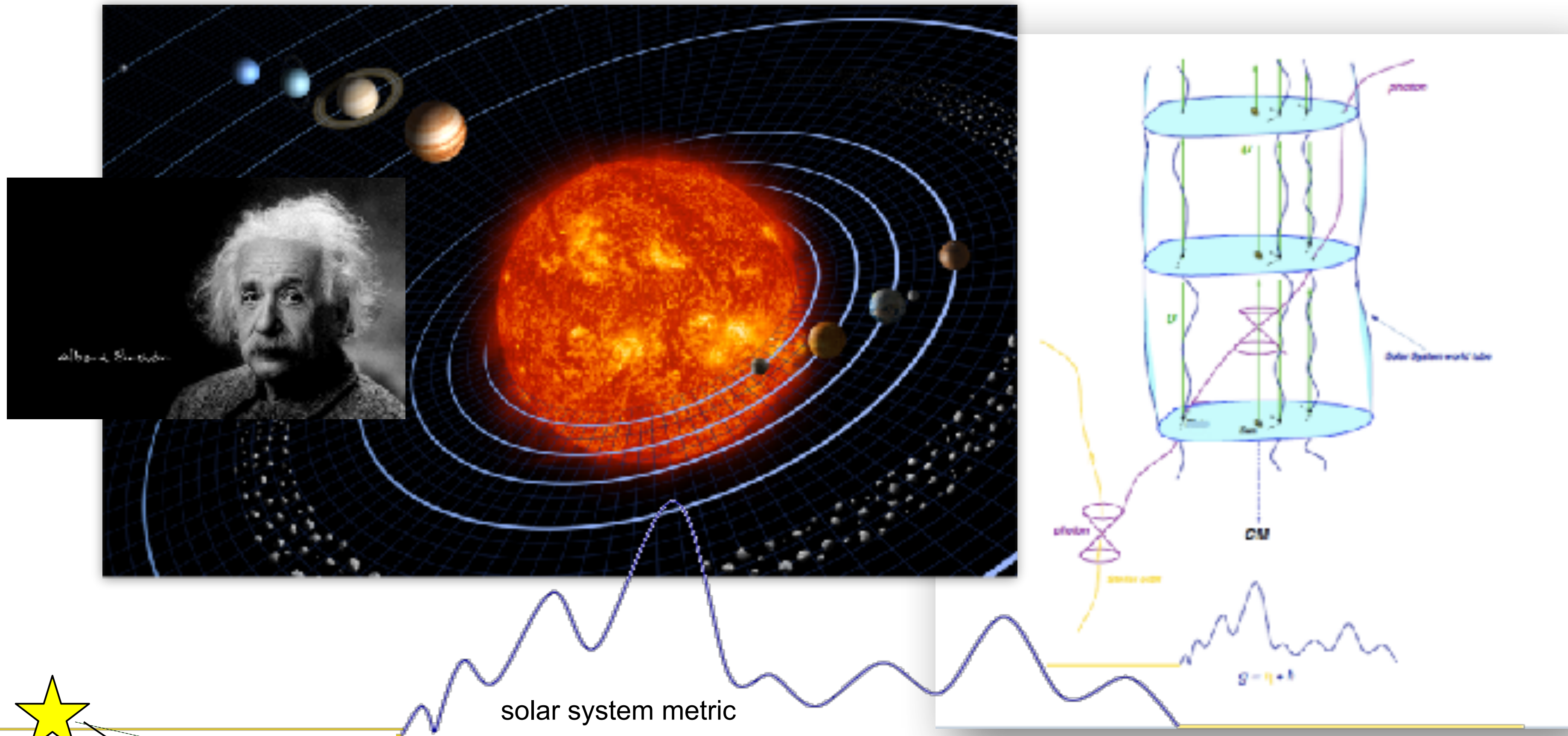

$$g = \eta + h$$

h pertubations at μ-**arcsec** due to the solar system bodies

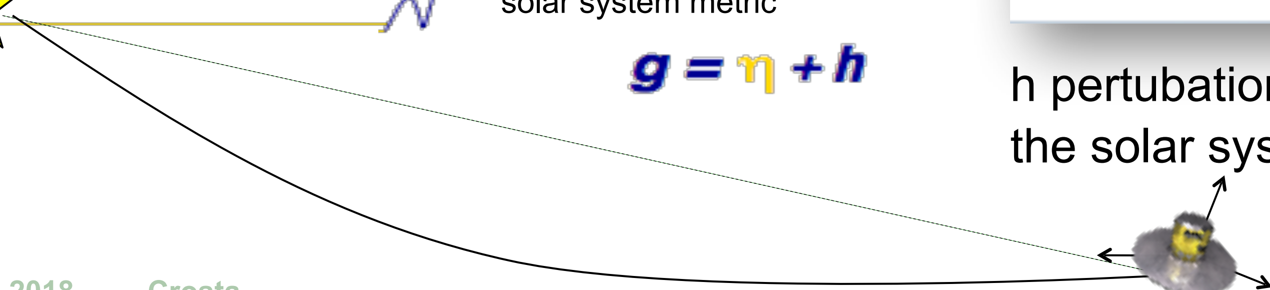

Our laboratory: the Solar System

micro-arcsecond accuracy+ dynamical gravitational fields=> relativistic models of light propagation:
RELATIVISTIC ASTROMETRY

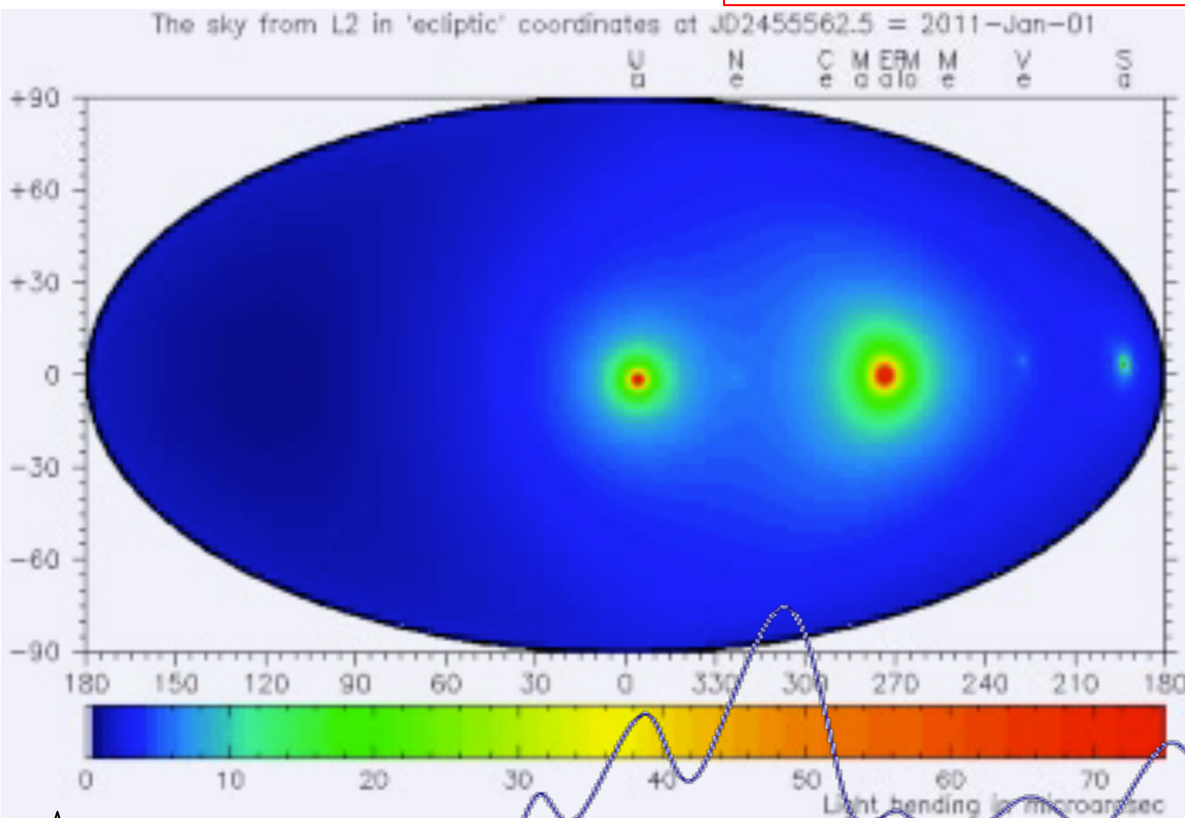

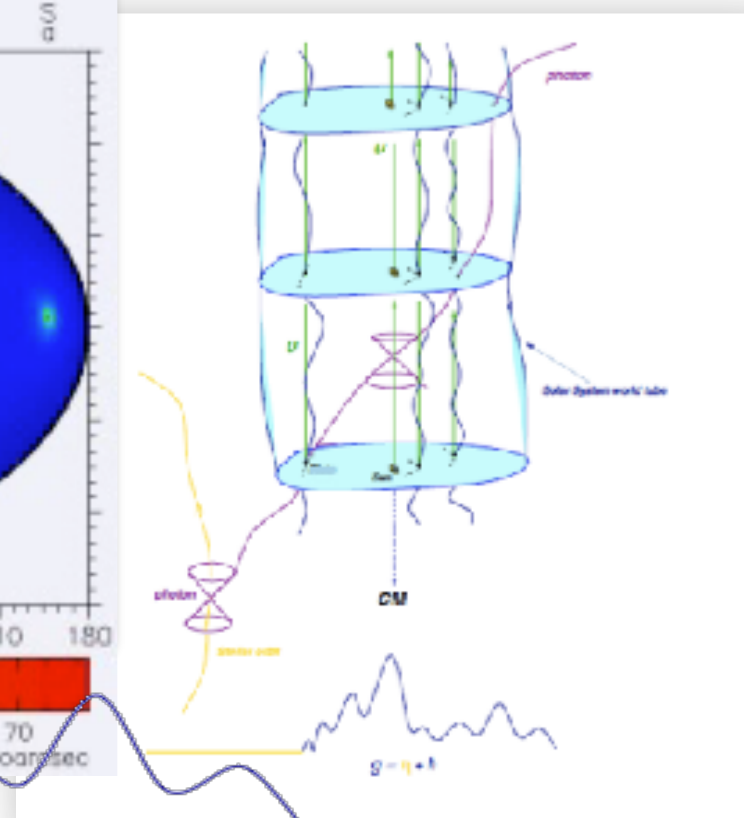

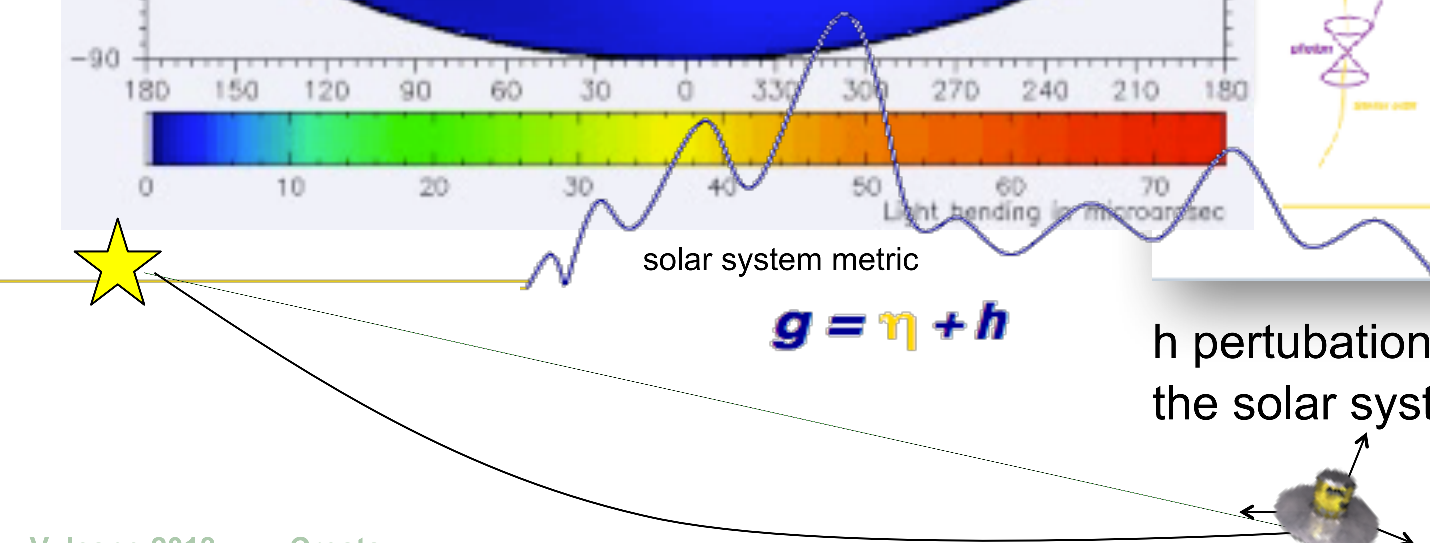

$$g = \eta + h$$

h pertubations at μ-**arcsec** due to the solar system bodies

Light crossing the metric of the Solar System

$$g_{\alpha\beta} = \eta_{\alpha\beta} + h_{\alpha\beta} + O(h^2)$$

$$|h_{\alpha\beta}| \ll 1$$

according to the Virial Theorem

$$|h_{\alpha\beta}| \leq U/c^2 \sim v^2/c^2 \rightarrow \varepsilon^2$$

~ v^2/c^2 ~ GM/rc^2 ~ mas accuracy

which requires determination of

g_{oo} even terms in ε, lowest order ε^2~mas

g_{oj} odd terms in ε, lowest order ε^3~μ-as

g_{ij} even terms in ε, lowest order ε^2~mas

Time variation of the order of $\epsilon |h_{\alpha\beta}|$

→ **IAU metric!**

$$k^\alpha k_\alpha = 0, \quad \frac{dk^\alpha}{d\lambda} + \Gamma^\alpha_{\rho\sigma} k^\rho k^\sigma = 0$$

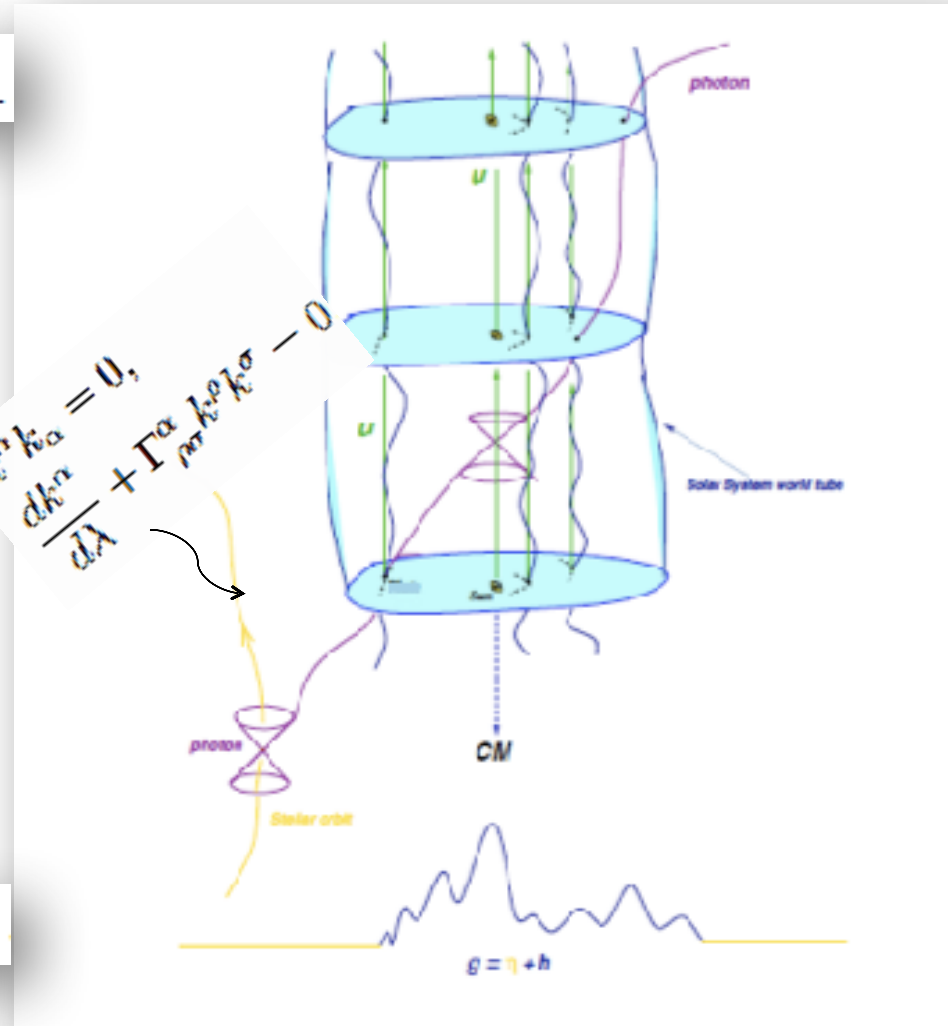

Detectable relativistic deflections at L2 at 1-PN level for grazing light ray

Body	$\delta\alpha_M$ (μas)	$\delta\alpha_Q$ (μas)
Sun	1.75×10^6	~ 1
Mercury	83	
Venus	493	
Earth	574	0.6
Moon	26	
Mars	116	0.2
Jupiter	16270	240
Saturn	5780	95
Uranus	2080	8
Neptune	2533	10

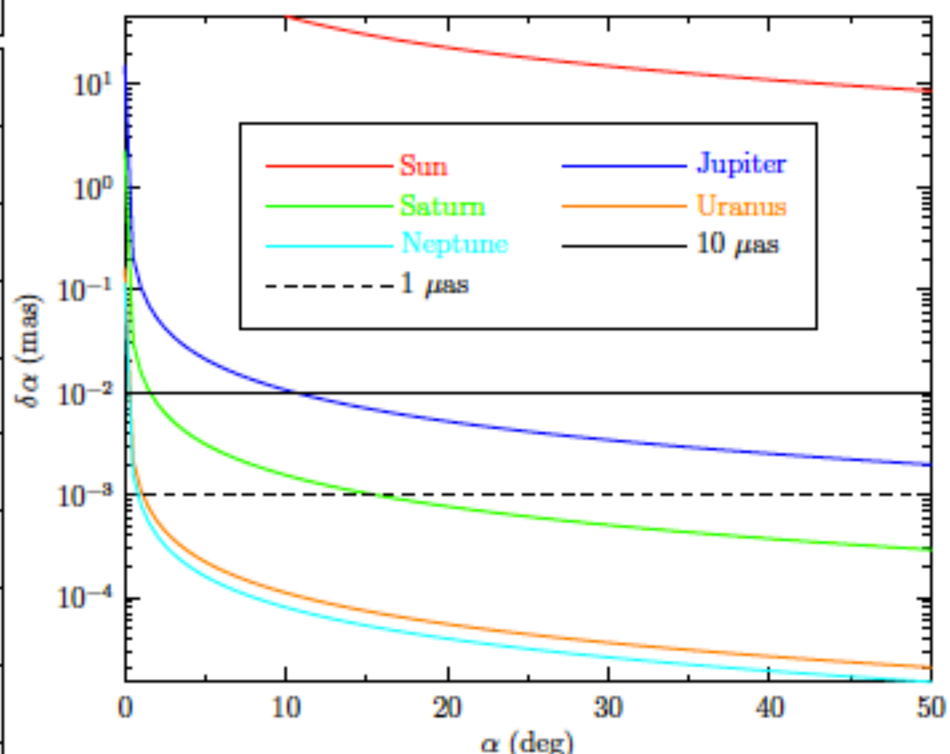

from the observer to the star through space-time: null geodesic

- ➢in tracing back light rays we need to keep consistency, at any level of approximations, with GR
- ➢this implies a new rendition of the astronomical observables and it may open, at the sub-muas level, a new detection window of many subtle relativistic effects naturally folded in the light while it propagates through the geometry of space-time up to the “local” observer

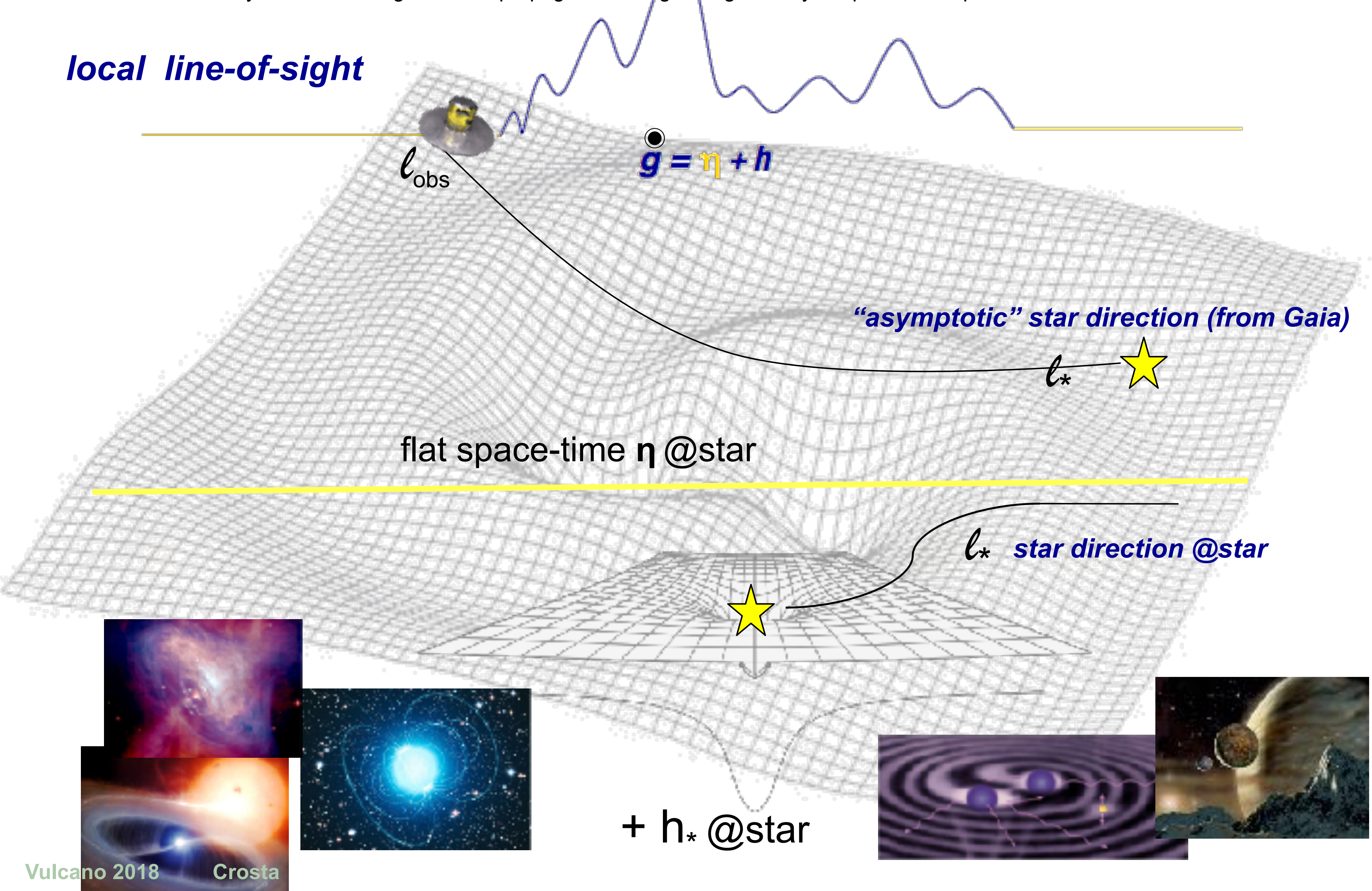

from the observer to the star through space-time: null geodesic

- ➢in tracing back light rays we need to keep consistency, at any level of approximations, with GR
- ➢this implies a new rendition of the astronomical observables and it may open, at the sub-muas level, a new detection window of many subtle relativistic effects naturally folded in the light while it propagates through the geometry of space-time up to the “local” observer

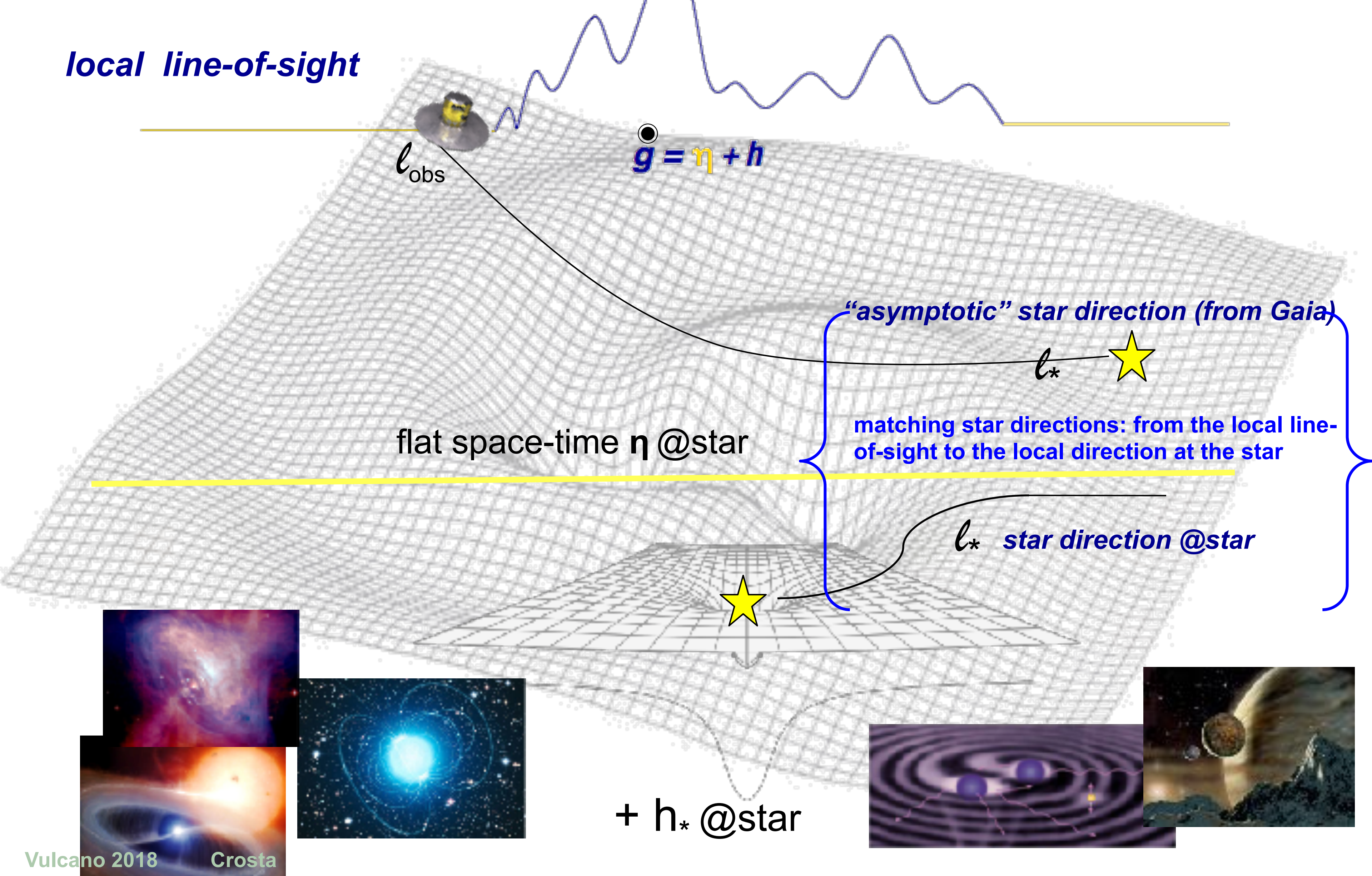

from the observer to the star through space-time: null geodesic

➢in tracing back light rays we need to keep consistency, at any level of approximations, with GR
➢this implies a new rendition of the astronomical observables and it may open, at the sub-muas level, a new detection window of many subtle relativistic effects naturally folded in the light while it propagates through the geometry of space-time up to the “local” observer

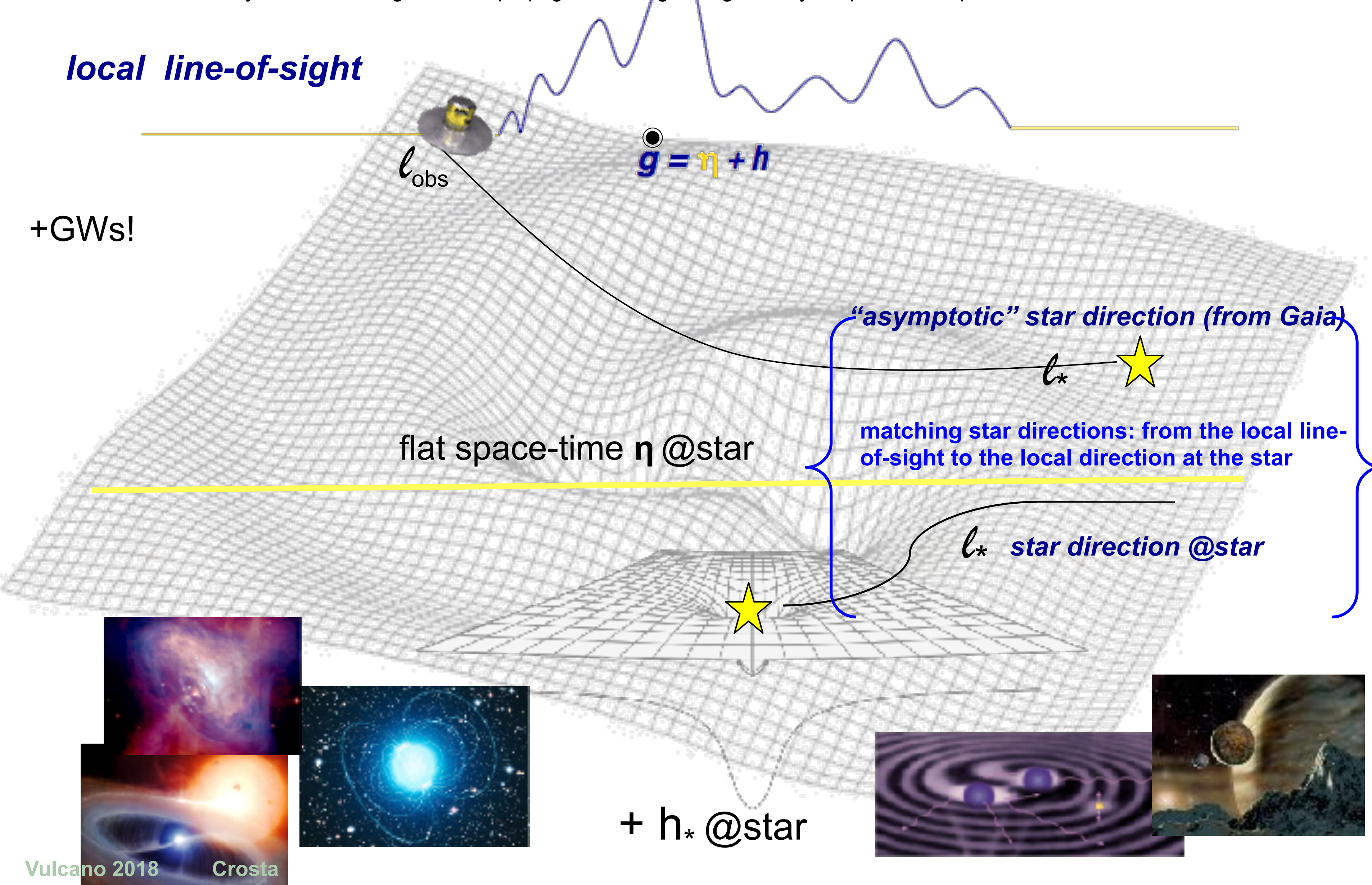

Gaia, CU3- REMAT: RElativistic Models And Tests

- The core processes of the astrometric pipeline is the so-called Global Astrometric Sphere Reconstruction, which uses global astrometric techniques on a subset of primary stars/QSO's to materialize the IC reference frame (ICRF).
- Given the absolute character of such reconstruction, the the Consortium constitued for the Gaia data reduction (DPAC) agreed to set up **two independent sphere solutions: AGIS and GSR**.
- GSR stands for Global Sphere Reconstruction (and Comparison), and its twofold goal is to provide the DPAC with an independent global sphere and to compare it to its AGIS (Astrometric Global Iterative Solution, baseline) analogue (GREM model)
- The theoretical model implemented in GSR is the RAMOD family (Relativistic Astrometric MODel) -> Astrometric Verification Unit (AVU, the 3rd fundamental component of the astrometric error budget) at the Italian data center (DPCT)

both models/solutions work on the same Gaia data: independent validation process

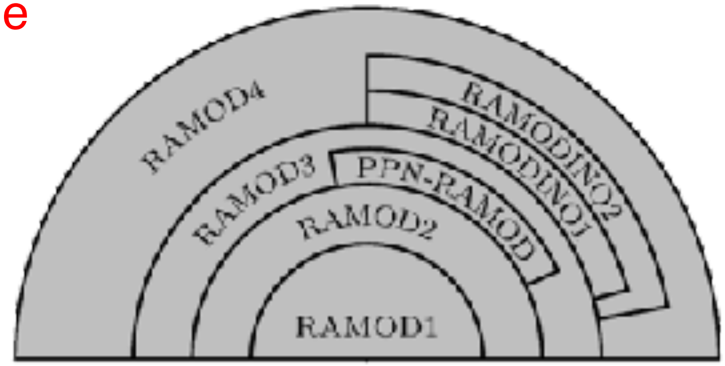

RAMOD is a framework of general relativistic astrometric models with increasing intrinsic accuracy, adapted to many different observer's settings, **interfacing numerical and analytical relativity**
RAMOD applies the measurement protocol (MP) in GR

Italian Data Processing Center

All Gaia operations activities (daily and cyclic) done in Italy are implemented at the DPCT, the Italian provided HW and SW operations system designed, built and run by ALTEC (To) and INAF-OATo for ASI.

DPCT was established through a specific ASI contract via a partnership between INAF-OATo and ALTEC S.p.A.

- **M. Castronuovo (RC, MLA-SC repr.)**
- **B. Negri (EOS Head)**

This is the only Data Processing Center, within the network of 6 DPCs dedicated to Gaia, which specializes in the treatment of the satellite astrometric data

The DPCT hosts the systems AVU:

Essential components of Gaia's astrometric error budget

- ❖ CCD-level precision and accuracy (Astrometric Instrument Monitoring - AIM)
- ❖ Accuracy at the Optical System level (Basic Angle Monitoring - BAM/AVU)
- ❖ Precision & accuracy on the celestial sphere (Global Sphere Reconstruction - GSR)

DPCT at full capacity. Current size about 500 TB of data.
Size at completion ~ 1.2 PB

- ❖ MoU CINECA-INAF

Italian Data Processing Center

All Gaia operations activities (daily and cyclic) done in Italy are implemented at the DPCT, the Italian provided HW and SW operations system designed, built and run by ALTEC (To) and INAF-OATo for ASI.

DPCT was established through a specific ASI contract via a partnership between INAF-OATo and ALTEC S.p.A.

- **M. Castronuovo (RC, MLA-SC repr.)**
- **B. Negri (EOS Head)**

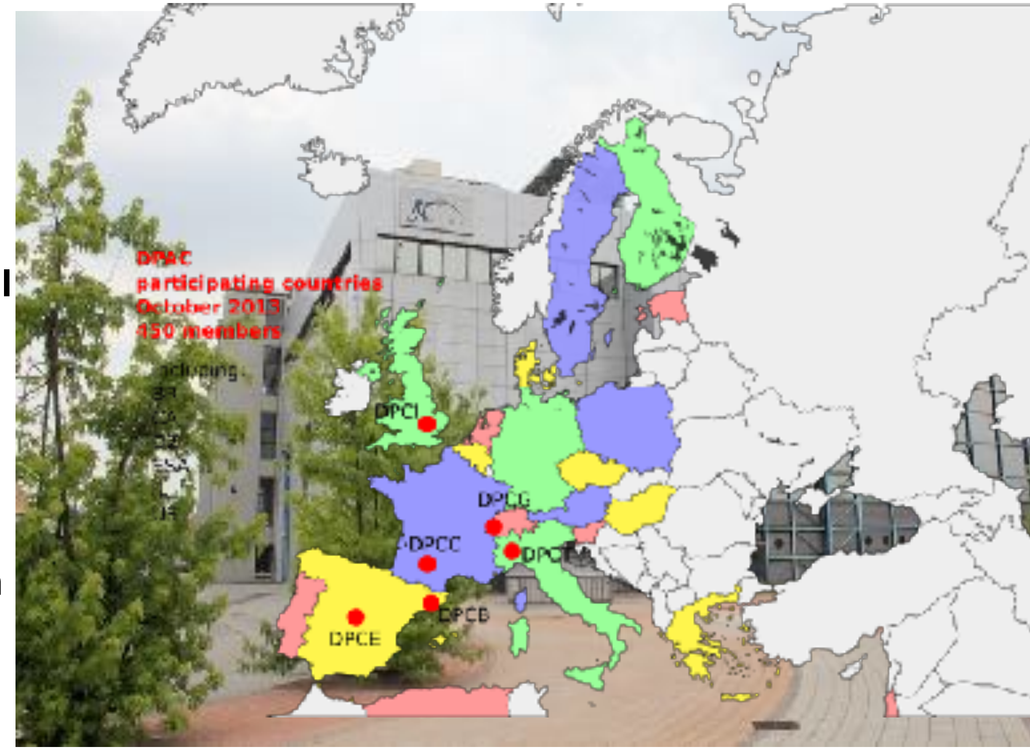

This is the only Data Processing Center, within the network of 6 DPCs dedicated to Gaia, which specializes in the treatment of the satellite astrometric data

The DPCT hosts the systems AVU:

Essential components of Gaia's astrometric error budget

- ❖ CCD-level precision and accuracy (Astrometric Instrument Monitoring - AIM)
- ❖ Accuracy at the Optical System level (Basic Angle Monitoring - BAM/AVU)
- ❖ Precision & accuracy on the celestial sphere (Global Sphere Reconstruction - GSR)

DPCT at full capacity. Current size about 500 TB of data.
Size at completion ~ 1.2 PB

- ❖ MoU CINECA-INAF

RAMOD vs GREM

RAMOD-like models aim to estimate the astrometric parameters of celestial objects from a well-defined set of relativistically measured quantity

$$\ell^\alpha = P^\alpha_\beta(u)k^\beta(\tau) \rightarrow \frac{d\ell^\alpha}{d\sigma} = F^\alpha(\partial_\beta h(x,y,z,t), \ell^i(\sigma(x)))$$

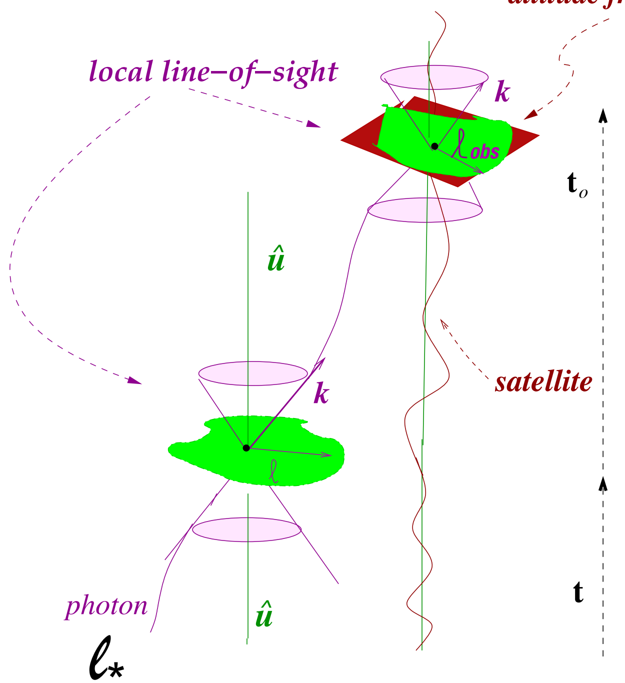

$\mathbf{x}_* = F(x_{obs}, g_{\mu\nu}, \ell_{obs}, E_a, \ldots.)$

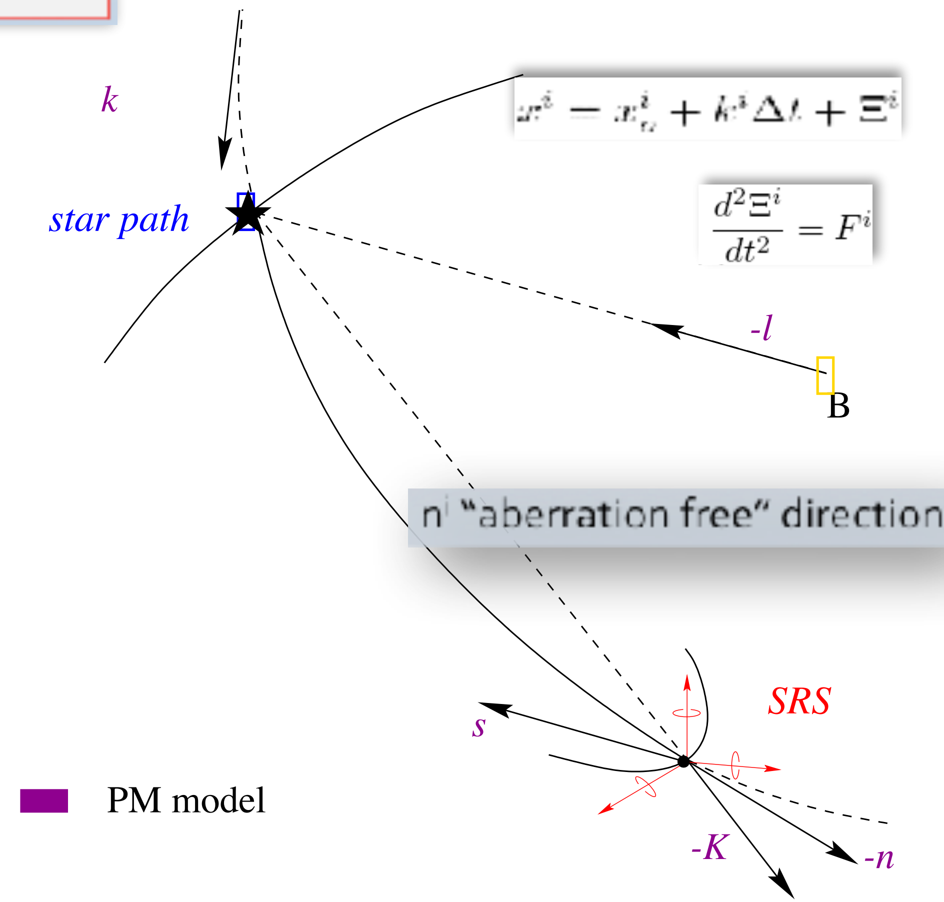

The RAMOD local-line-of-sight is not exactly equal to the light direction used in the semi-classical approximation

$$\bar{l}^i = n^i\left(1-\frac{h_{00}}{2}\right) + \mathcal{O}\left(\frac{v^4}{c^4}\right)$$

aberrated (gravitational) direction

$h_{00}/2 \approx U/c^2$ (local potential)[IAU solution]

→ **100 μas!**

from the local line-of-sight to the star "position"

	☉	☉+♃	☉+♃+♄	☉+♃+♄+♅	☉+♃+♄+♅+♆
distance ~ 1 pc					
d (AU)	206261.338	206259.698	206259.216	206259.142	206259.054
p_i ('')	1.00001775	1.00002571	1.00002804	1.00002840	1.00002883
$p_\odot - p_i$ (μarcsec)		-7.95	-10.29	-10.65	-11.07
$\Delta\psi_i$ (μarcsec)		-8.00	-10.30	-10.60	-11.10
distance ~ 10 pc					
d (AU)	2062283.55	2062120.14	2062072.27	2062064.94	2062056.3
p_i ('')	0.10001777	0.10002569	0.10002802	0.10002837	0.10002879
$p_\odot - p_i$ (μarcsec)		7.93	10.25	10.60	11.02
$\Delta\psi_i$ (μarcsec)		-8.00	-10.30	-10.60	-11.00
distance ~ 100pc					
d (AU)	20589921.6	20573645.4	20568881.5	20568152.5	20567292.3
p_i ('')	0.01001777	0.01002569	0.01002801	0.01002837	0.01002879
$p_\odot - p_i$ (μarcsec)		-7.93	-10.25	-10.60	-11.02
$\Delta\psi_i$ (μarcsec)		-7.99	-10.30	-10.60	-11.00
distance ~ 1000 pc					
d (AU)	202664764	201098829	200644596	200575248	200493473
p_i ('')	0.00101776	0.00102569	0.00102801	0.00102837	0.00102879
$p_\odot - p_i$ (μarcsec)		-7.93	-10.25	-10.60	-11.02
$\Delta\psi_i$ (μarcsec)		-7.99	-10.30	-10.60	-11.00
distance ~ 10000 pc					
d (AU)	1751489760	1641052370	1611285280	1609051510	1603803810
p_i ('')	0.00011777	0.00012569	0.00012801	0.00012819	0.00012861
$p_\odot - p_i$ (μarcsec)		-7.93	-10.25	-10.42	-10.84
$\Delta\psi_i$ (μarcsec)		-7.99	-10.30	-10.60	-11.00

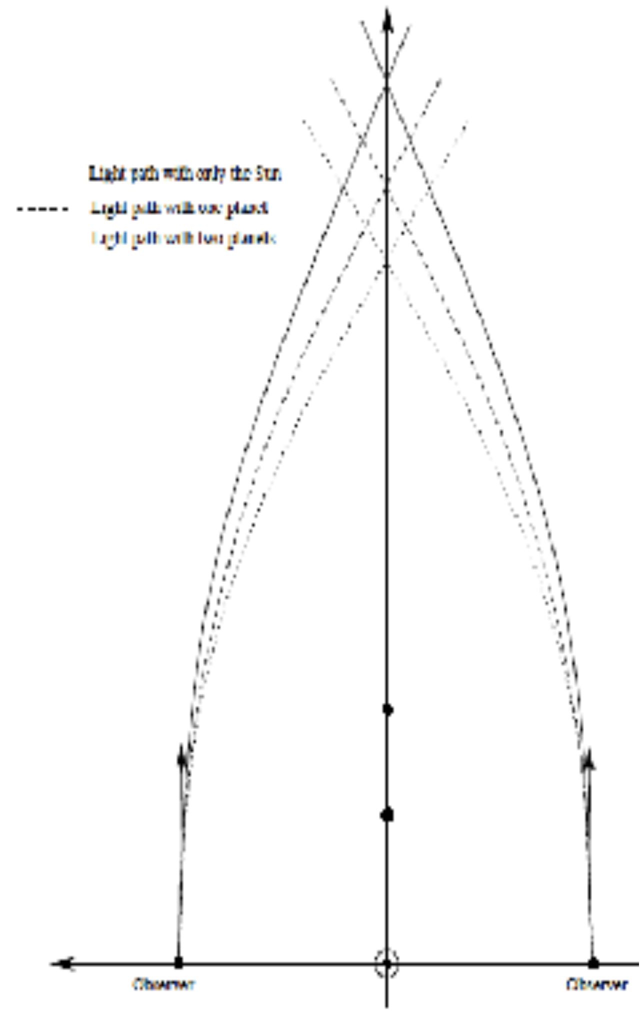

relative error in mag with no planets
(only the Sun) for d=10kpc ⇒ $\sigma_{m-M} \approx 2\ \sigma_d / d \approx 0.2$ mag!

from the local line-of-sight to the star "position"

	⊙	⊙+♃	⊙+♃+♄	⊙+♃+♄+♅	⊙+♃+♄+♅+♆
		distance ~ 1 pc			
d (AU)	206261.338	206259.698	206259.216	206259.142	206259.054
p_i (″)	1.00001775	1.00002571	1.00002804	1.00002840	1.00002883
$p_\odot - p_i$ (μarcsec)		-7.95	-10.29	-10.65	-11.07
$\Delta\psi_i$ (μarcsec)		-8.00	-10.30	-10.60	-11.10
		distance ~ 10 pc			
d (AU)	2062283.55	2062120.14	2062072.27	2062064.94	2062056.3
p_i (″)	0.10001777	0.10002569	0.10002802	0.10002837	0.10002879
$p_\odot - p_i$ (μarcsec)		7.93	10.25	10.60	11.02
$\Delta\psi_i$ (μarcsec)		-8.00	-10.30	-10.60	-11.00
		distance ~ 100pc			
d (AU)	20589921.6	20573645.4	20568881.5	20568152.5	20567292.3
p_i (″)	0.01001777	0.01002569	0.01002801	0.01002837	0.01002879
$p_\odot - p_i$ (μarcsec)		-7.93	-10.25	-10.60	-11.02
$\Delta\psi_i$ (μarcsec)		-7.99	-10.30	-10.60	-11.00
		distance ~ 1000 pc			
d (AU)	202664764	201098829	200644596	200575248	200493473
p_i (″)	0.00101776	0.00102569	0.00102801	0.00102837	0.00102879
$p_\odot - p_i$ (μarcsec)		-7.93	-10.25	-10.60	-11.02
$\Delta\psi_i$ (μarcsec)		-7.99	-10.30	-10.60	-11.00
		distance ~ 10000 pc			
d (AU)	1751489760	1641052370	1611285280	1609051510	1603803810
p_i (″)	0.00011777	0.00012569	0.00012801	0.00012819	0.00012861
$p_\odot - p_i$ (μarcsec)		-7.93	-10.25	-10.42	-10.84
$\Delta\psi_i$ (μarcsec)		-7.99	-10.30	-10.60	-11.00

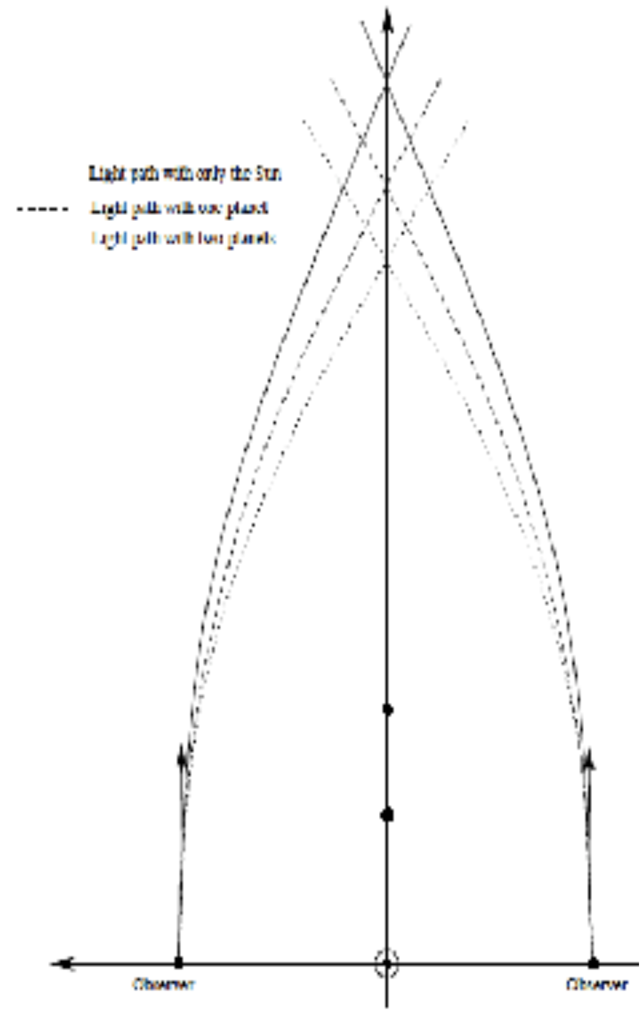

relative error in mag with no planets
(only the Sun) for d=10kpc

$\sigma_{m-M} \approx 2\,\sigma_d/d \approx 0.2$ mag!

The astrometric observable in RAMOD/AVU

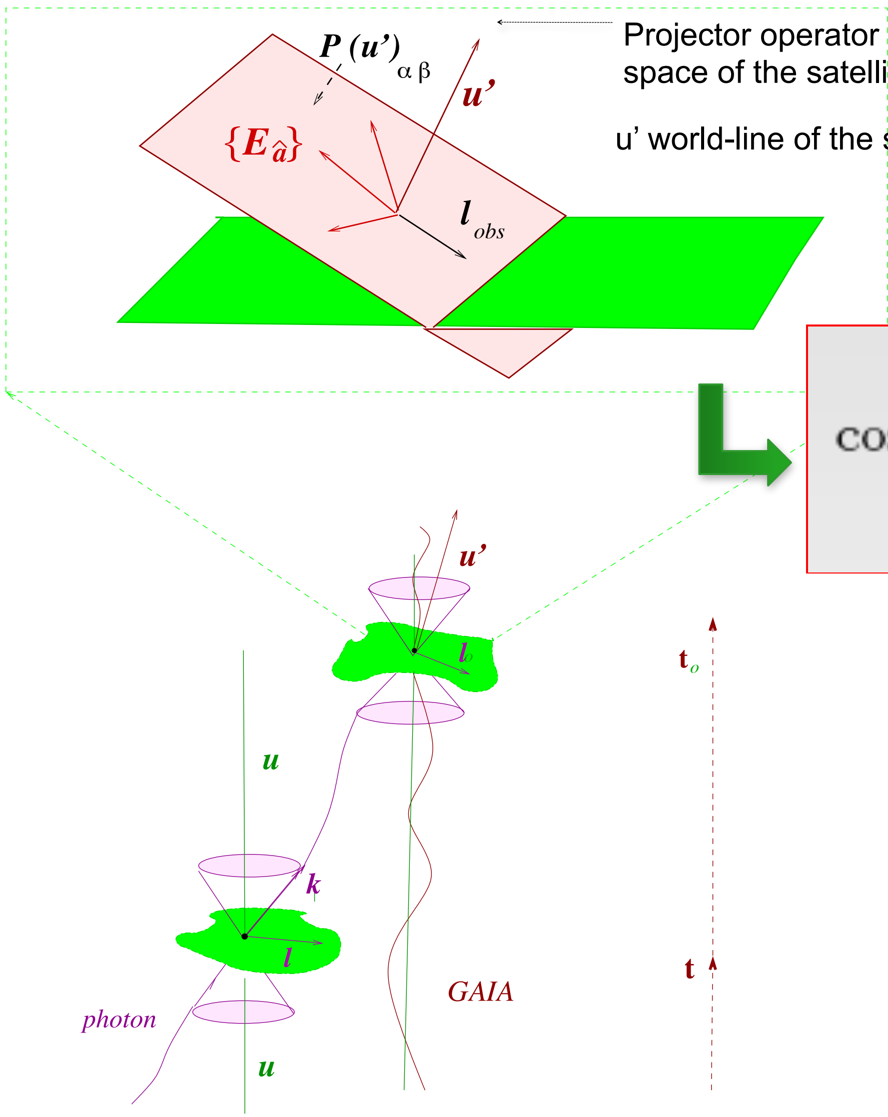

$E_\alpha^{\ \beta}$ "attitude tetrad"-> ESSENTIAL to define the boundary condition

$$\cos\psi_{(E_{\hat{a}},\ell_{obs})} \equiv \mathbf{e}_{\hat{a}} = \frac{P(u')_{\alpha\beta}\ell_{obs}^{\alpha}\boldsymbol{E}^{\beta}_{\hat{a}}}{(P(u')_{\alpha\beta}k^{\alpha}k^{\beta})^{1/2}}$$

Observation equation

The astrometric observable in RAMOD/AVU

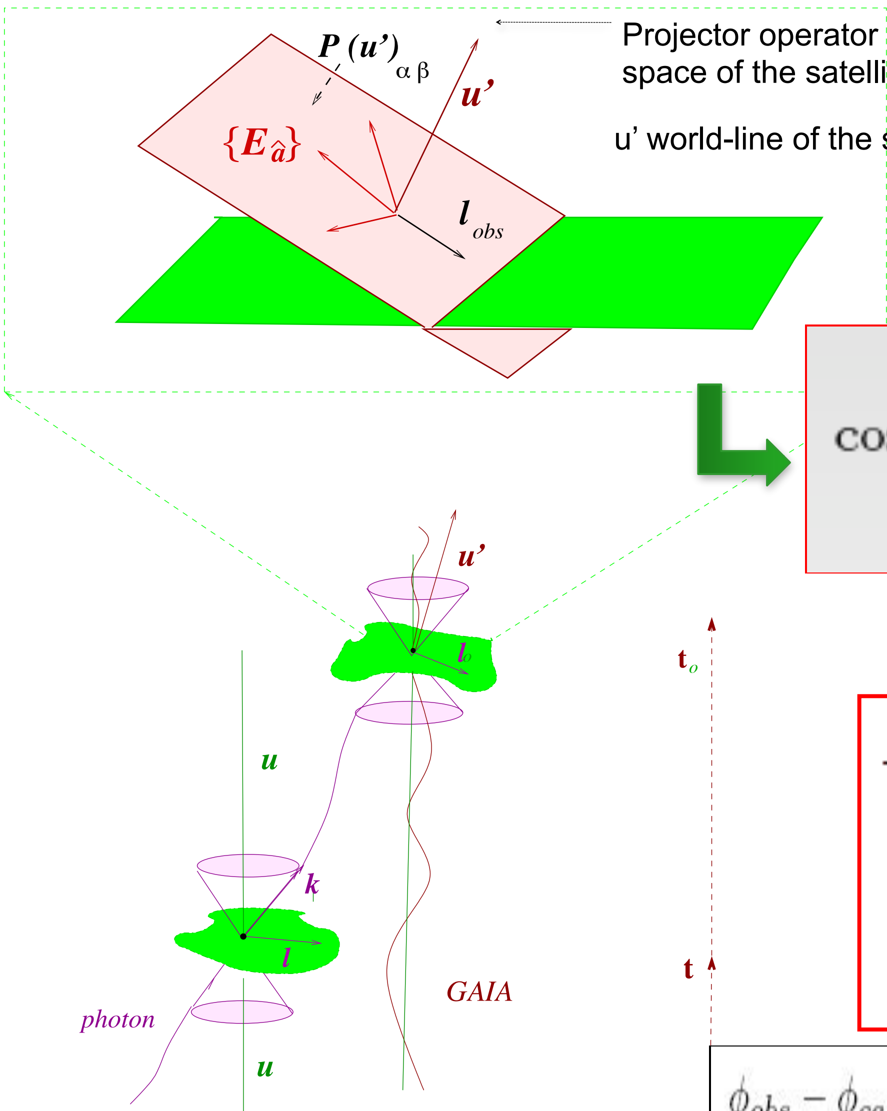

$E_\alpha{}^\beta$ "attitude tetrad"-> ESSENTIAL to define the boundary condition

$$\cos\psi_{(E_{\hat{a}},\ell_{obs})} \equiv \mathbf{e}_{\hat{a}} = \frac{P(u')_{\alpha\beta}\,\ell^{\alpha}_{obs}\,\boldsymbol{E}^{\beta}_{\hat{a}}}{(P(u')_{\alpha\beta}k^{\alpha}k^{\beta})^{1/2}}$$

Observation equation

$$-\sin\phi\, d\phi = \underbrace{\frac{\partial F}{\partial \alpha_*}\delta\alpha_* + \frac{\partial F}{\partial \delta_*}\delta\delta_* + \frac{\partial F}{\partial \varpi_*}\delta\varpi_* + \cdots}_{\text{Astrometric parameters}} \; \sum_{ij}\frac{\partial F}{\partial \sigma_i^{(j)}}\delta\sigma_i^{(j)} + \sum_i \frac{\partial F}{\partial c_i}\delta c_i + \frac{\partial F}{\partial \gamma}\delta\gamma + \cdots$$

$$\phi_{obs} - \phi_{calc}$$

All derivatives are calculated at appropriate "catalog" values

The concept of the Global Sphere Reconstruction

$$\cos\phi = F\left(\underbrace{\alpha_*, \delta_*, \varpi_*, \mu_{\alpha*}, \mu_{\delta*}}_{\text{Astrometric parameters}}, \underbrace{\sigma_1^{(1)}, \sigma_2^{(1)}, \sigma_3^{(1)}, \sigma_1^{(3)}, \sigma_2^{(3)}, \sigma_3^{(3)}}_{\text{Attitude parameters}}, \underbrace{c_1, c_2, \dots}_{\text{Instrument}} \underbrace{\gamma, \dots}_{\text{Global}}\right)$$

Solving the linearized GSR sphere in the Least-Squares sense

Known **Unknown** **Unknown**

$$\sin\psi_i^{(1)}\,\Delta\psi_i^{(1)} = \frac{\partial f}{\partial\alpha_i}\Delta\alpha_i + \frac{\partial f}{\partial\delta_i}\Delta\delta_i + \frac{\partial f}{\partial\pi_i}\Delta\pi_i + \cdots + \frac{\partial f}{\partial\gamma}\Delta\gamma$$

$$\sin\psi_i^{(2)}\,\Delta\psi_i^{(2)} = \frac{\partial f}{\partial\alpha_i}\Delta\alpha_i + \frac{\partial f}{\partial\delta_i}\Delta\delta_i + \frac{\partial f}{\partial\pi_i}\Delta\pi_i + \cdots + \frac{\partial f}{\partial\gamma}\Delta\gamma$$

• • • • • •

$$\sin\psi_i^{(n)}\,\Delta\psi_i^{(n)} = \frac{\partial f}{\partial\alpha_i}\Delta\alpha_i + \frac{\partial f}{\partial\delta_i}\Delta\delta_i + \frac{\partial f}{\partial\pi_i}\Delta\pi_i + \cdots + \frac{\partial f}{\partial\gamma}\Delta\gamma$$

1 obs. $\Rightarrow$ 1 condition eq.

(linearized) system of solution with dimensions $\sim 10^{10} \times 10^{8}$

parallelized implementation of the LSQR iterative algorithm (Paige & Saunders, 1982) tailored for the sphere solution problem

The concept of the Global Sphere Reconstruction

$$\cos\phi = F\Big(\underbrace{\alpha_*,\delta_*,\varpi_*,\mu_{\alpha*},\mu_{\delta*}}_{\text{Astrometric parameters}},\underbrace{\sigma_1^{(1)},\sigma_2^{(1)},\sigma_3^{(1)},\sigma_1^{(3)},\sigma_2^{(3)},\sigma_3^{(3)}}_{\text{Attitude parameters}},\underbrace{c_1,c_2,\ldots}_{\text{Instrument}},\underbrace{\gamma,\ldots}_{\text{Global}}\Big)$$

Crosta et al. Phys. Rev. D 96,104030, 2017 "*General relativistic observable for gravitational astrometry in the context of the Gaia mission and beyond*"

Solving the linearized GSR sphere in the Least-Squares sense

Known — Unknown — Unknown

$$\sin\psi_i^{(1)}\,\Delta\psi_i^{(1)} = \frac{\partial f}{\partial\alpha_i}\Delta\alpha_i + \frac{\partial f}{\partial\delta_i}\Delta\delta_i + \frac{\partial f}{\partial\pi_i}\Delta\pi_i + \cdots + \frac{\partial f}{\partial\gamma}\Delta\gamma$$

$$\sin\psi_i^{(2)}\,\Delta\psi_i^{(2)} = \frac{\partial f}{\partial\alpha_i}\Delta\alpha_i + \frac{\partial f}{\partial\delta_i}\Delta\delta_i + \frac{\partial f}{\partial\pi_i}\Delta\pi_i + \cdots + \frac{\partial f}{\partial\gamma}\Delta\gamma$$

• • • • • •

$$\sin\psi_i^{(n)}\,\Delta\psi_i^{(n)} = \frac{\partial f}{\partial\alpha_i}\Delta\alpha_i + \frac{\partial f}{\partial\delta_i}\Delta\delta_i + \frac{\partial f}{\partial\pi_i}\Delta\pi_i + \cdots + \frac{\partial f}{\partial\gamma}\Delta\gamma$$

1 obs. ⇒ 1 condition eq.

(linearized) system of solution with dimensions $\sim 10^{10}\times 10^{8}$

parallelized implementation of the LSQR iterative algorithm (Paige & Saunders, 1982) tailored for the sphere solution problem

Fundamental Physics tests via global astrometry

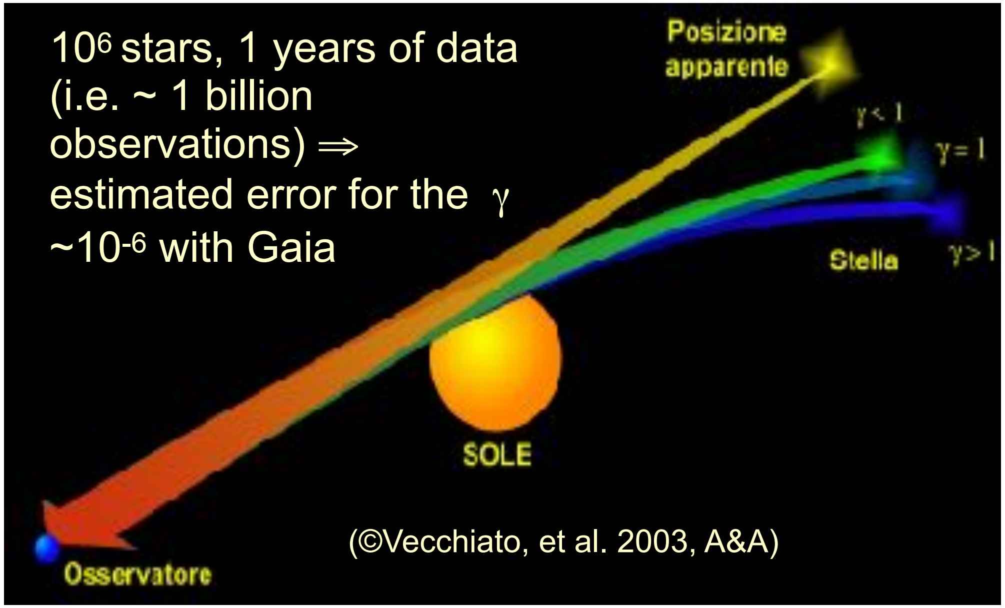

deviations from GR depends on the particular scalar-tensor theory adopted (quantum theory of gravity, verification of inflationary models, violation of the principle of equivalence, constancy of the physical constants, low-energy limits of string theories, accelerated cosmological expansion, Galaxy cluster dynamics, Galaxy rotation curves and DM halos, etc.)

→ *given the number of celestial objects (a real Galilean method applied on the sky!) and directions involved (the whole celestial sphere!), the largest experiment in General Relativity ever made with astrometric methods (since 1919) from space*

A massive repetition of the Eddington et al. astrometric test of GR with 21st century technology, thank to the interfacing of analytical&numerical relativity methods!

with **DR2** too many systematic errors, final calibrations including bright stars will improve the measurements of deviation from one

Demonstration Run:1 million primary sources, whole mag range, 5 years, blind simulation

The AVU-GSR sphere reconstruction
(the 3rd fundamental component of the astrometric error budget)

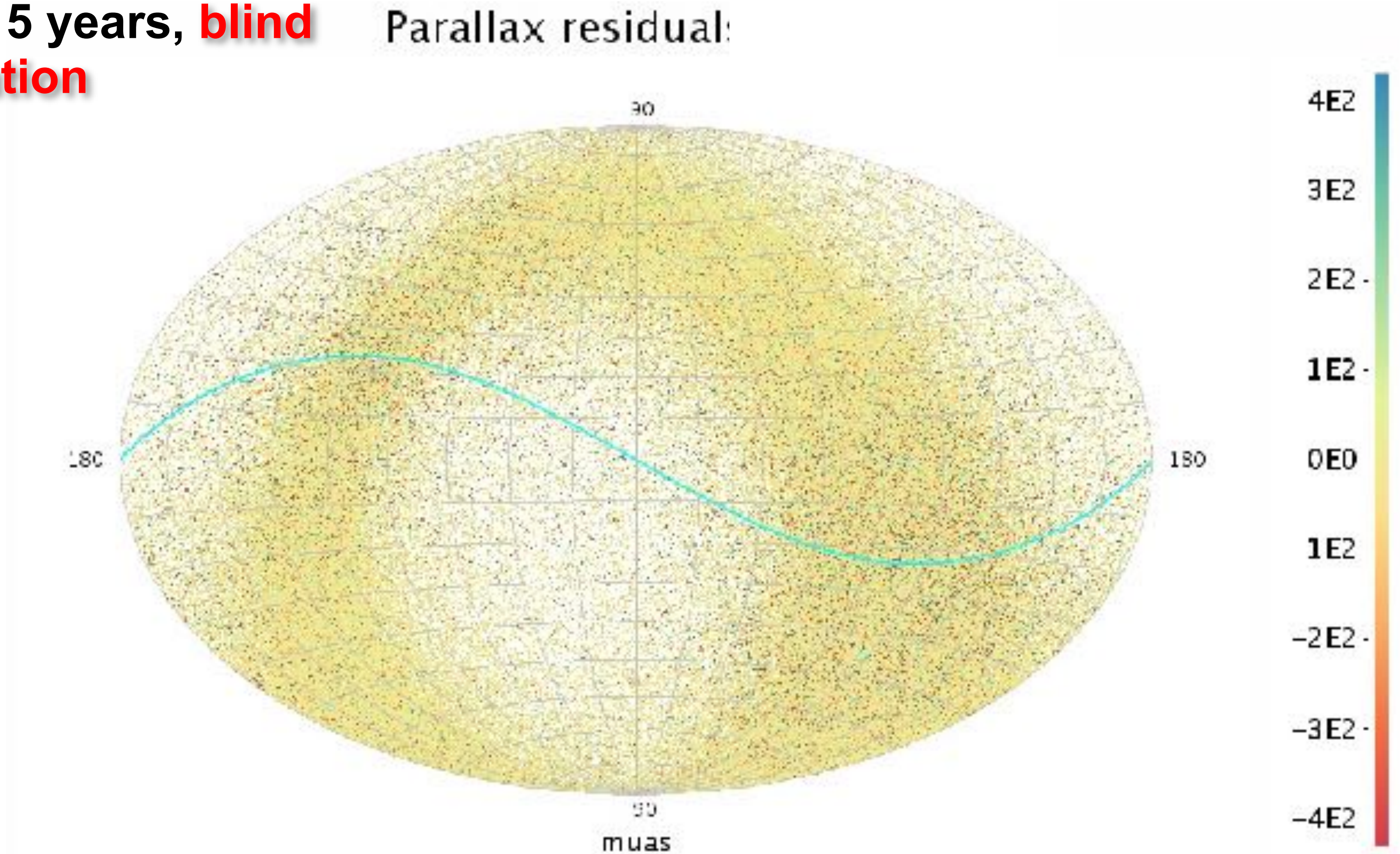

Courtesy of Bucciarelli, Lattanzi, Vecchiato

(From Vecchiato, MGL, Bucciarelli,…, GAIA-C3-TN-INAF-AVE-027-01, 26 Oct 17; A&A, 2018, submitted)

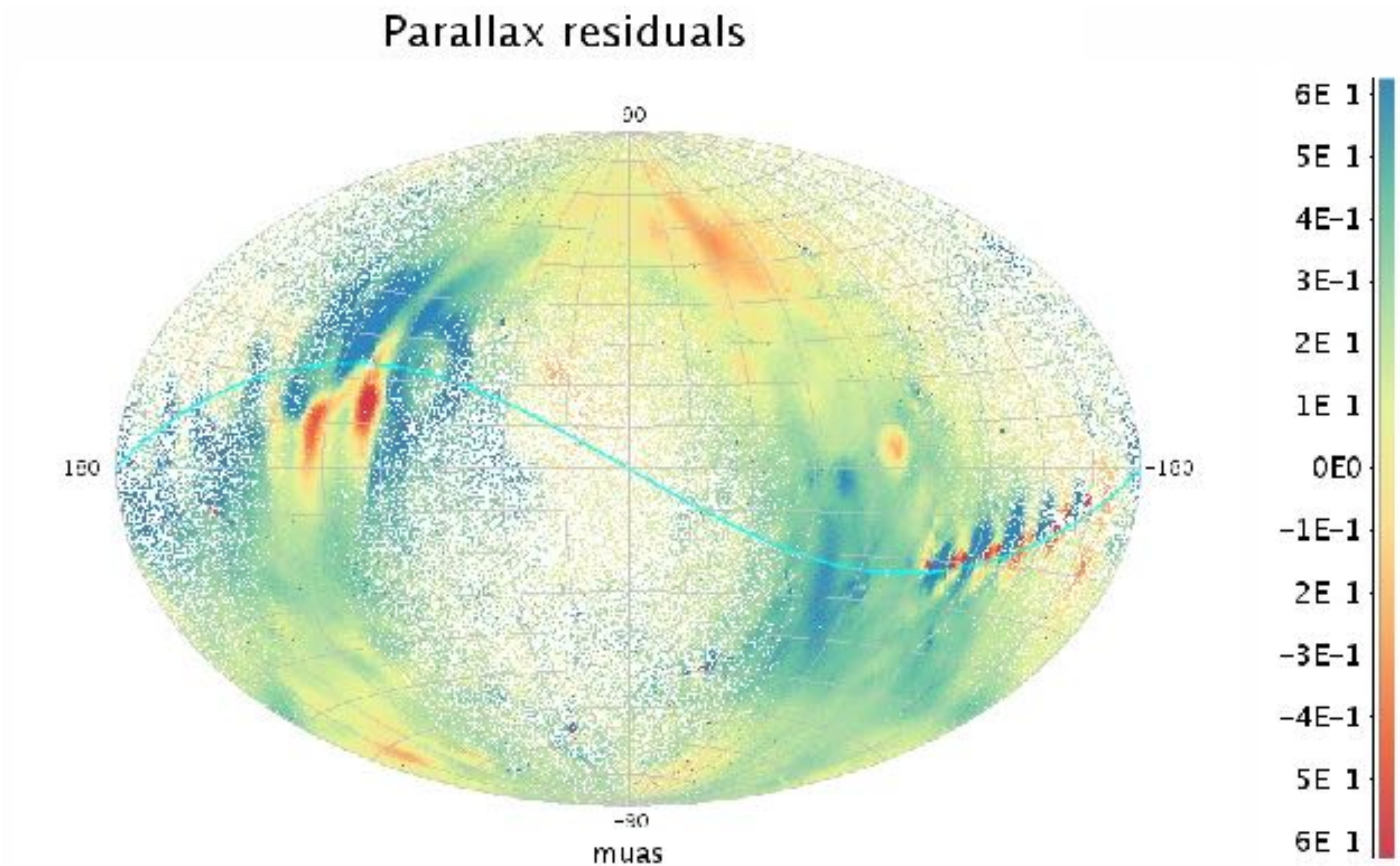

Courtesy of Bucciarelli, Lattanzi, Vecchiato

(From Vecchiato, MGL, Bucciarelli,…, GAIA-C3-TN-INAF-AVE-027-01, 26 Oct 17; A&A, 2018, submitted)

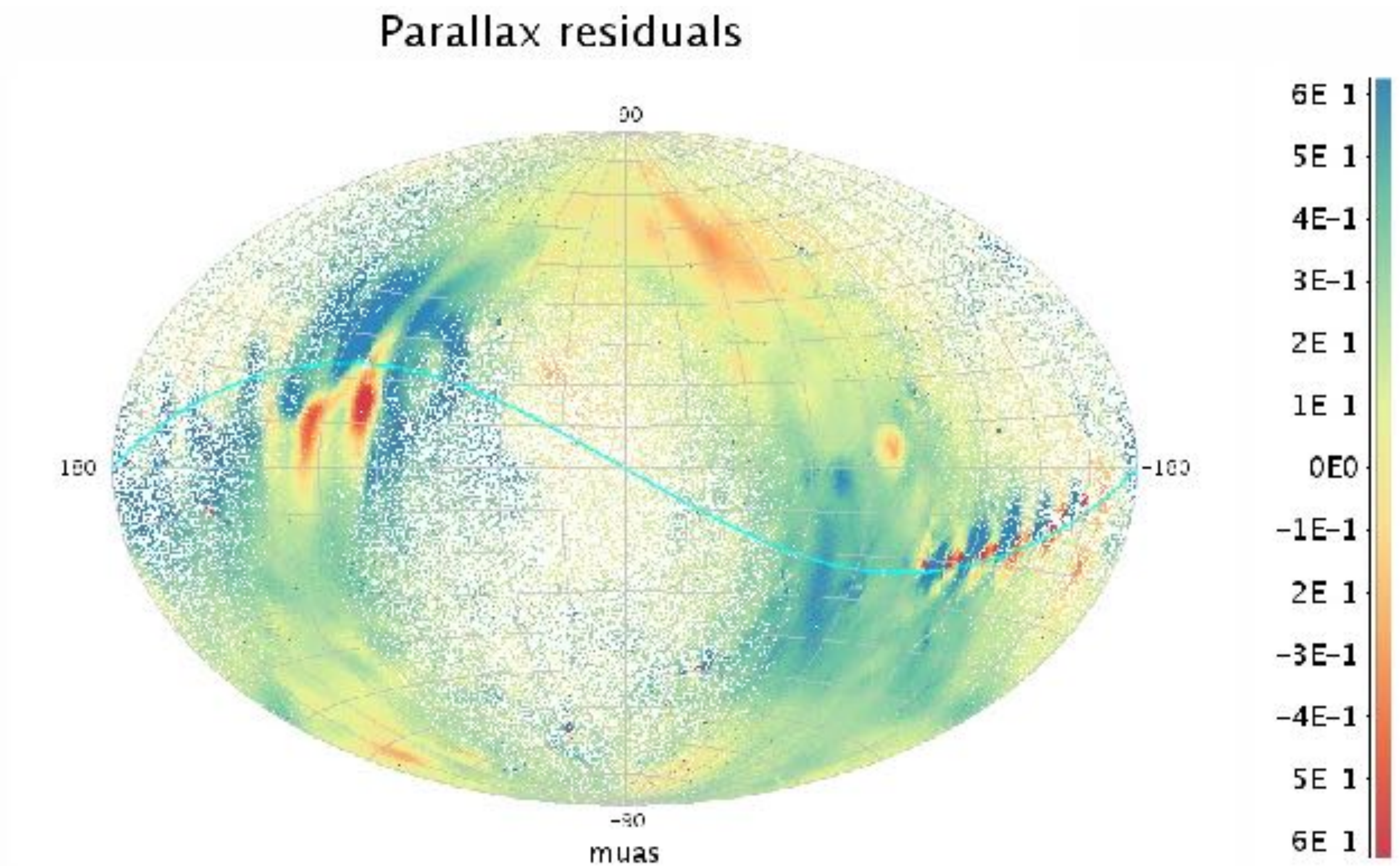

Bertone et al. A&A, v. 608, id.A83, 2017, Application of time transfer functions to *Gaia*'s global astrometry - Validation on DPAC simulated *Gaia*-like observations->TTF/GREM comparison

Courtesy of Bucciarelli, Lattanzi, Vecchiato

(From Vecchiato, MGL, Bucciarelli,…, GAIA-C3-TN-INAF-AVE-027-01, 26 Oct 17; A&A, 2018, submitted)

✓ Stressing the point

The Gaia-like observer is positioned inside the Solar System, a **<u>weak gravitational regime which turns out to be "strong" when one has to perform high accurate measurements</u>**

➢ Any discrepancy between the relativistic models, if it can not be attributed to errors of different nature, will mean either a limit in the modeling/interpretation - that a correct application of GR should fix - and therefore a validation of GR, or, maybe, a clue that we need to refine our approach to GR

- Independent relativistic astrometric model;
- Independent relativistic attitude model;
- Independent (iterative) solution method (all-unknowns solved at once);
- Direct calculation of variances of Primary solution (possibility of covariances!)
- At first comparison, common set of initial primary stars and instrument model;
- GSR compares to AGIS for verification at CU3 level (all-sky)

➢ all the goals of Gaia will not be achieved without the correct characterization and exploitation of the ``relativistic'' astrometric data.

GAREQ (GAia Relativistic Experiment on Quadrupole) (light deflection by Jupiter’s quadrupole)

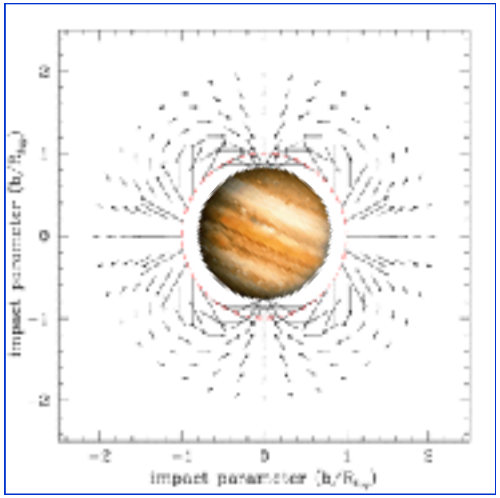

“q-effect”

Crosta, M., Mignard, F. (2006,**CQGr, 23, 4853**)
Crosta, et al. (2008, **GAIA-C3-TN-INAF-MTC-003-1)**

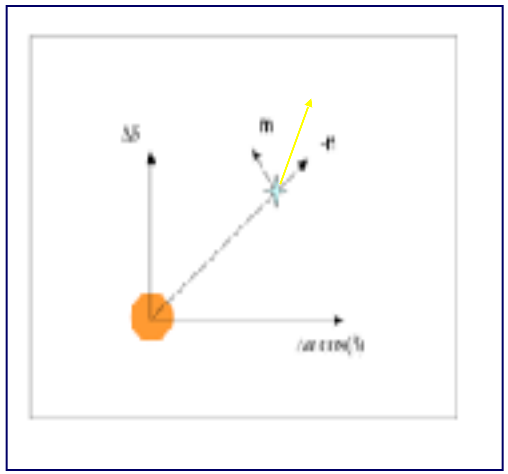

aim: first quantitative measurement of the gravitational potential due to a non-spherical lens

$$\Delta\Phi_1 = \frac{2(1+\gamma)M}{b}\left[1 + J_2\frac{R^2}{b^2}\left(1 - 2(\mathbf{n}\cdot\mathbf{z})^2 - (\mathbf{t}\cdot\mathbf{z})^2\right)\right]$$

$$\Delta\Phi_2 = \frac{4(1+\gamma)M J_2 R^2}{b^3}(\mathbf{m}\cdot\mathbf{z})(\mathbf{n}\cdot\mathbf{z})$$

$$\Delta\Phi = \Delta\Phi_1\mathbf{n} + \Delta\Phi_2\mathbf{m},$$

further validation of GR-> screening of alternative theories, confirmation of multipolar patterns of the gravitational lens generated by galaxy clusters provided that GR works as expected

Differential Astrometry in the GAREQ scenario: Q-DIFF

collaborators: U, Abbas B. Bucciarelli, M. G. Lattanzi, R. Morbidelli, D. Busonero, A. Vecchiato & R. Messineo

Figures: courtesy of M.G.Lattanzi

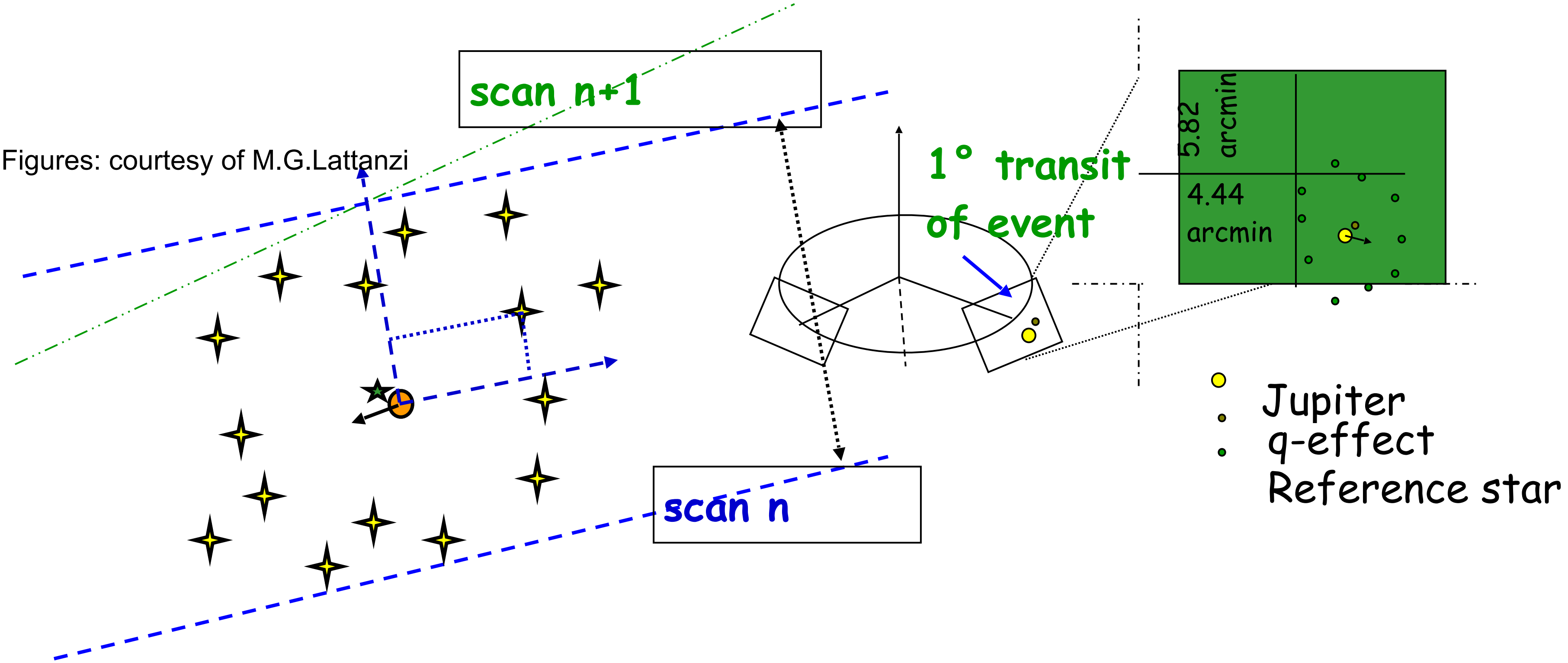

Differential Astrometry in the GAREQ scenario: Q-DIFF

collaborators: U, Abbas B. Bucciarelli, M. G. Lattanzi, R. Morbidelli, D. Busonero, A. Vecchiato & R. Messineo

Figures: courtesy of M.G.Lattanzi

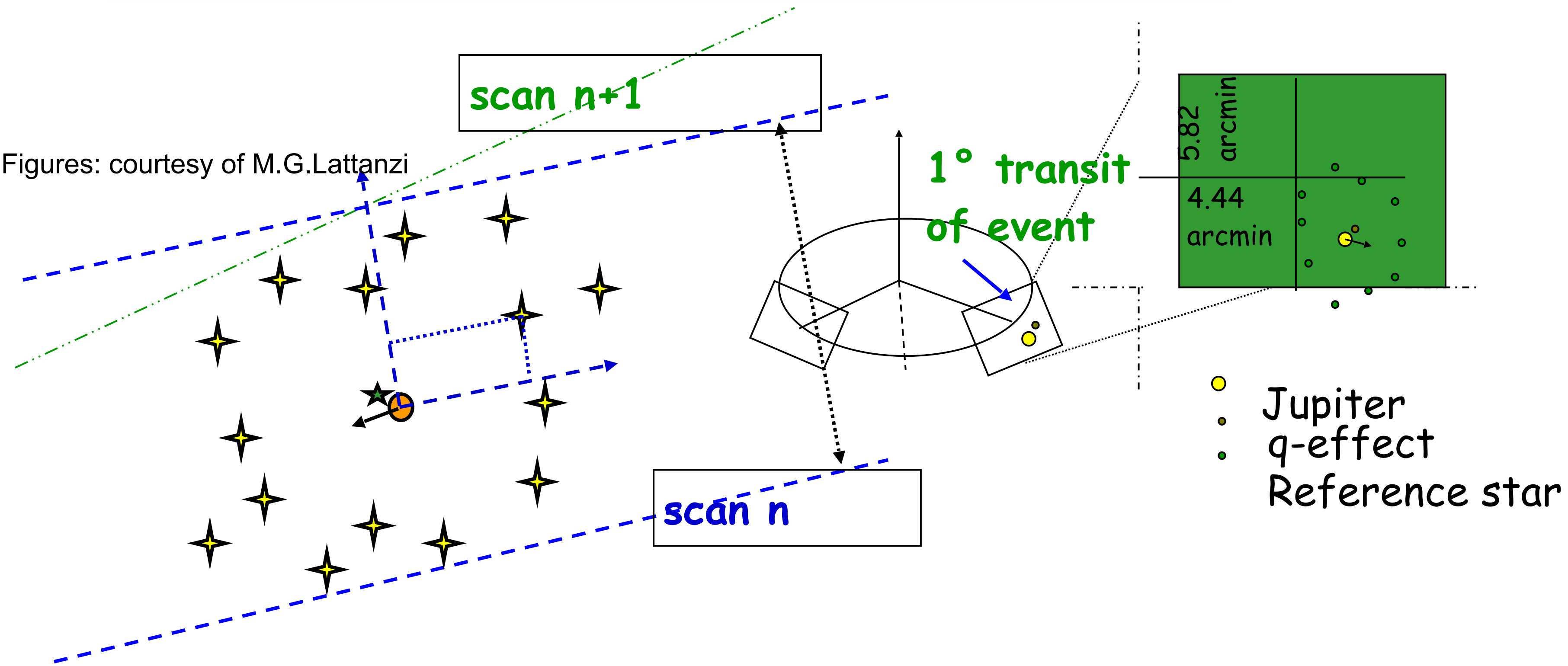

(On the same subject we have a multi-epoch, multi-orbit HST proposal – PI S. Casertano (STScI). Executed successfully, under reduction)

->#Gaia spin axis orientation optimised to catch a star close to the limb of Jupiter in 2017 for a precise light deflection measurement.

- Initial spin axis orientation decided 2014 to maximise measurement success
- Spin phase adjustment 8 Feb 2017
- Scan-law change for GAREQ event (spin phase change is 82.5º)

Observation of the first GAREQ event

At the beginning of 2017, towards the end of February 2017, Gaia provided measurements for 31 bright reference stars (G <13 mag) all lying within a field of 0.8x1.3 degs surrounding a target star (G= 12.68 mag) of particular interest.

The target star was seen a total of 26 times over a 2 month period out of which we use 15 transits over a short time interval of a couple of days surrounding the observation at closest approach

Credit: Mignard

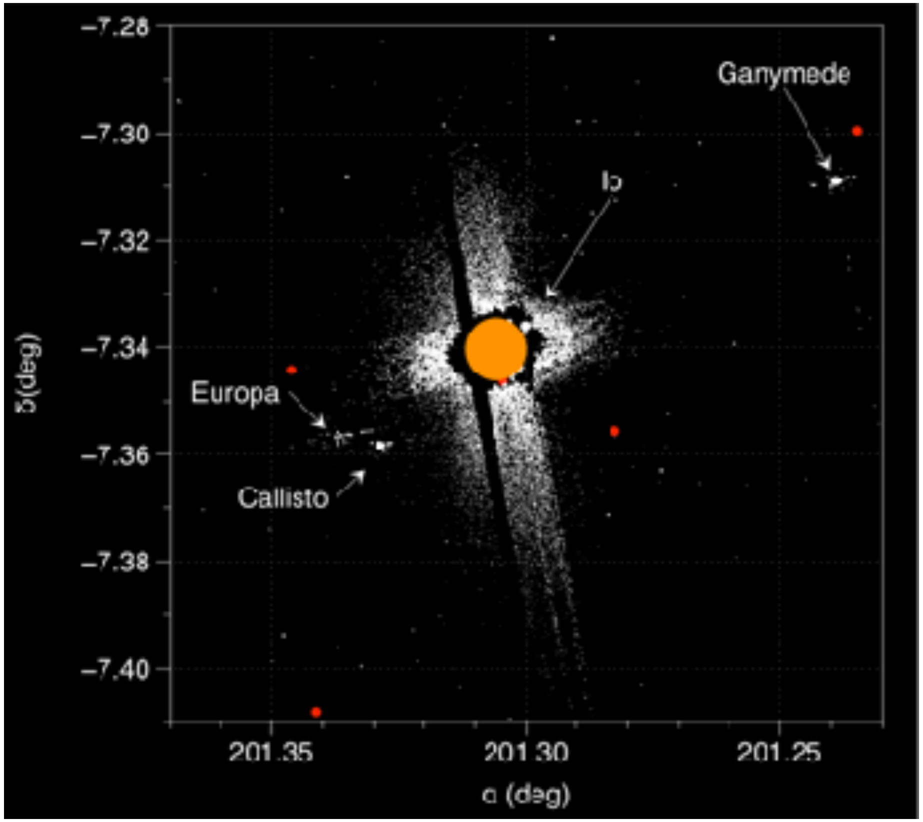

Observation of GAREQ event

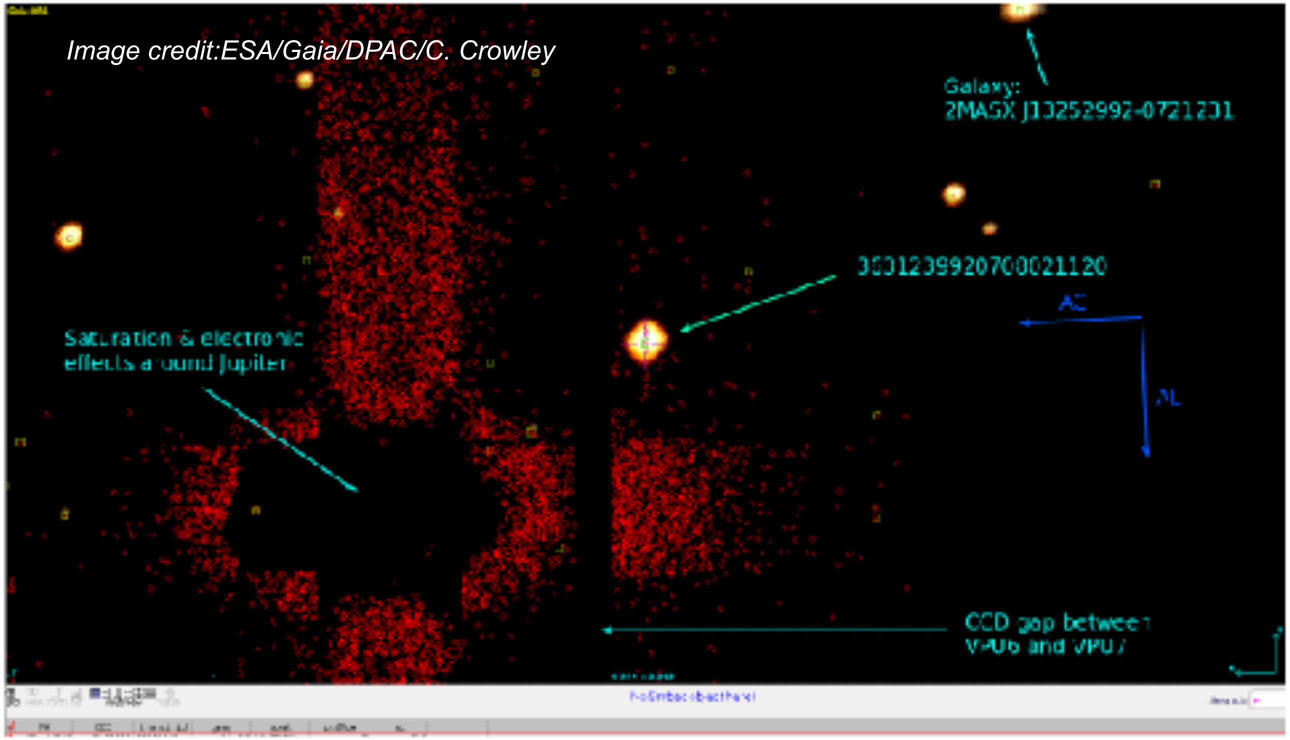

Scene around the target star successfully detected onboard during a transit on 2017-02-22T19:08:12.954 (UTC) at a predicted angular distance of 67.65” from Jupiter's limb. Note the gap between the detectors in CCD rows 6 and 7. Whilst Jupiter was observed in row 6, one of the measured bright star happened to be scanned in row 7.

Star field on different transits

diifferential astrometry to adjust all the frames to a common frame by means of translations, rotations and possible distortion terms if necessary

Image credit:ESA/Gaia/DPAC

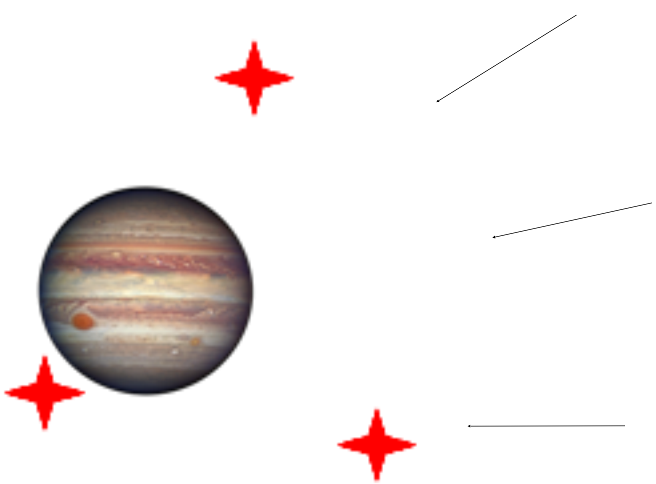

Star field on different transits

diifferential astrometry to adjust all the frames to a common frame by means of translations, rotations and possible distortion terms if necessary

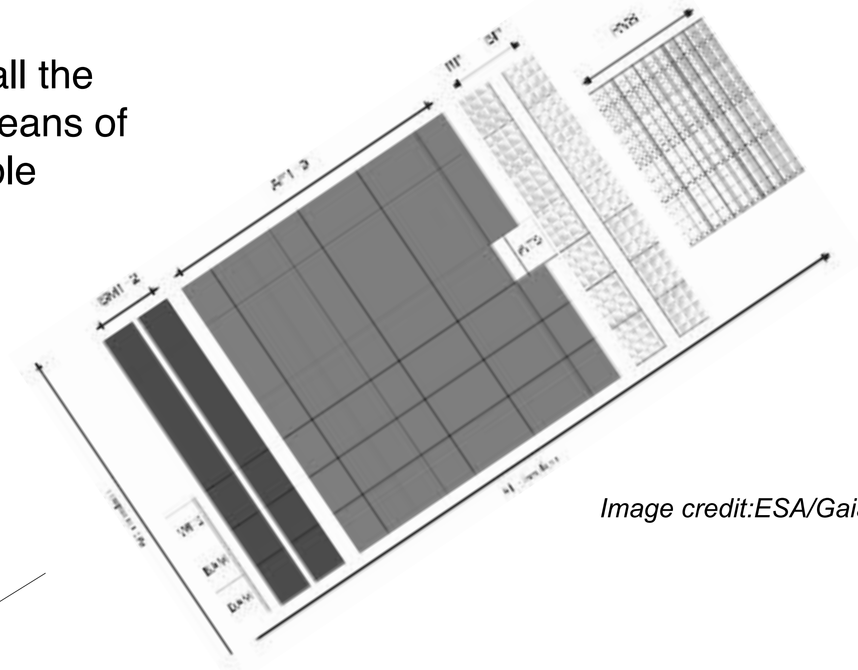

Image credit:ESA/Gaia/DPAC

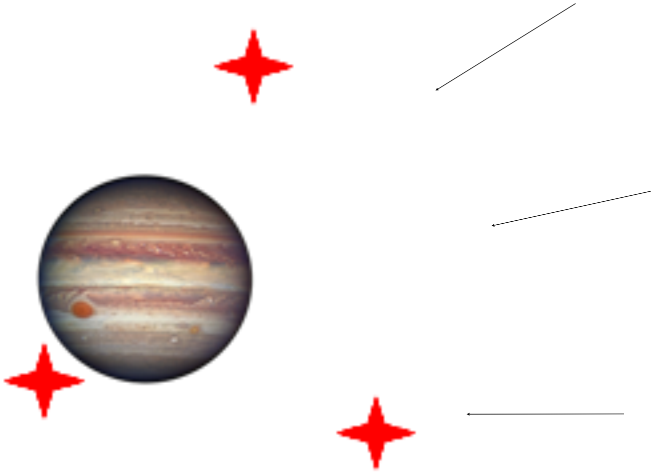

Star field on different transits

diifferential astrometry to adjust all the frames to a common frame by means of translations, rotations and possible distortion terms if necessary

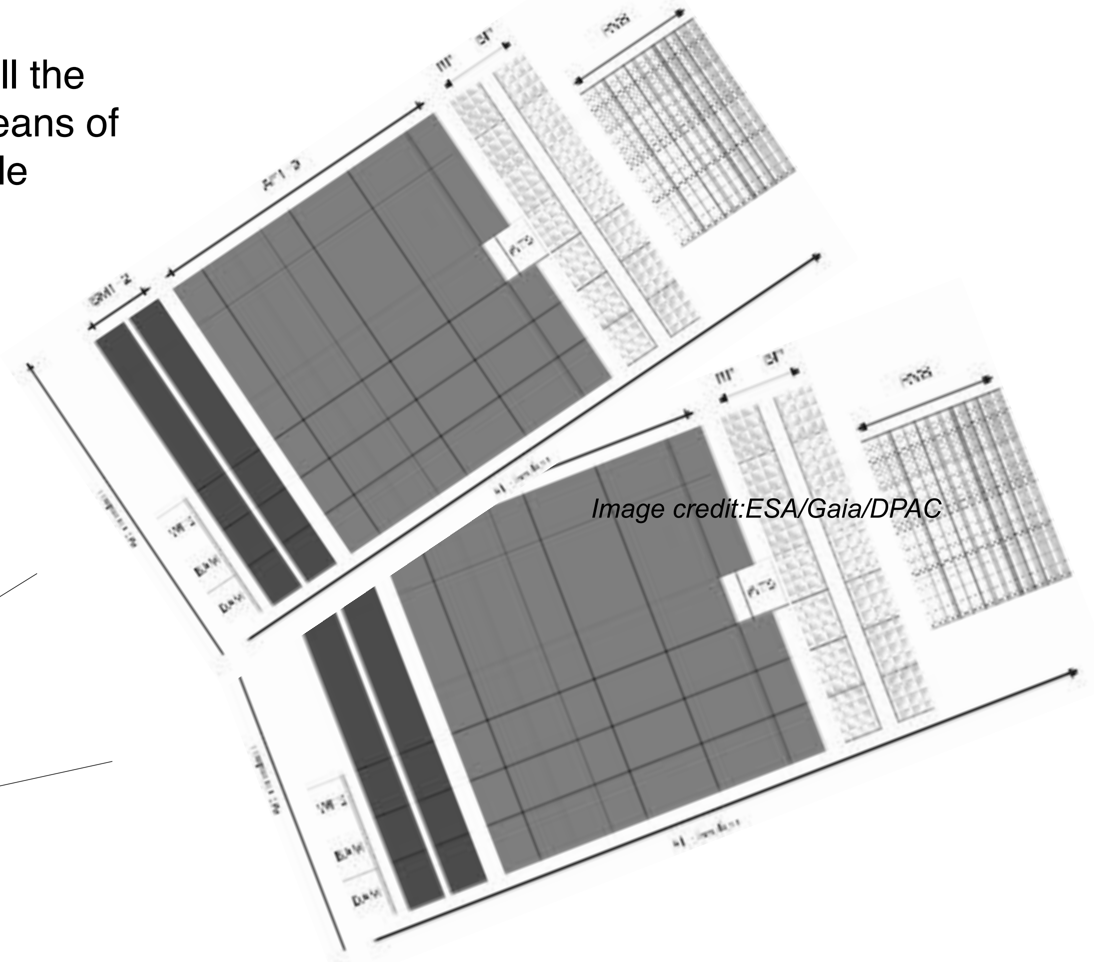

Image credit:ESA/Gaia/DPAC

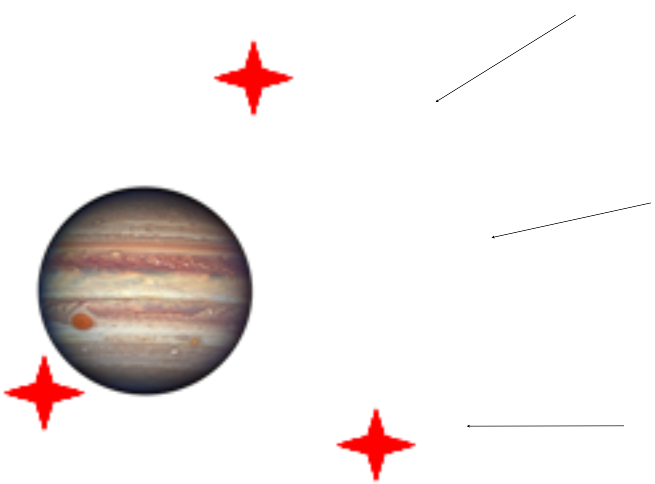

Star field on different transits

diifferential astrometry to adjust all the frames to a common frame by means of translations, rotations and possible distortion terms if necessary

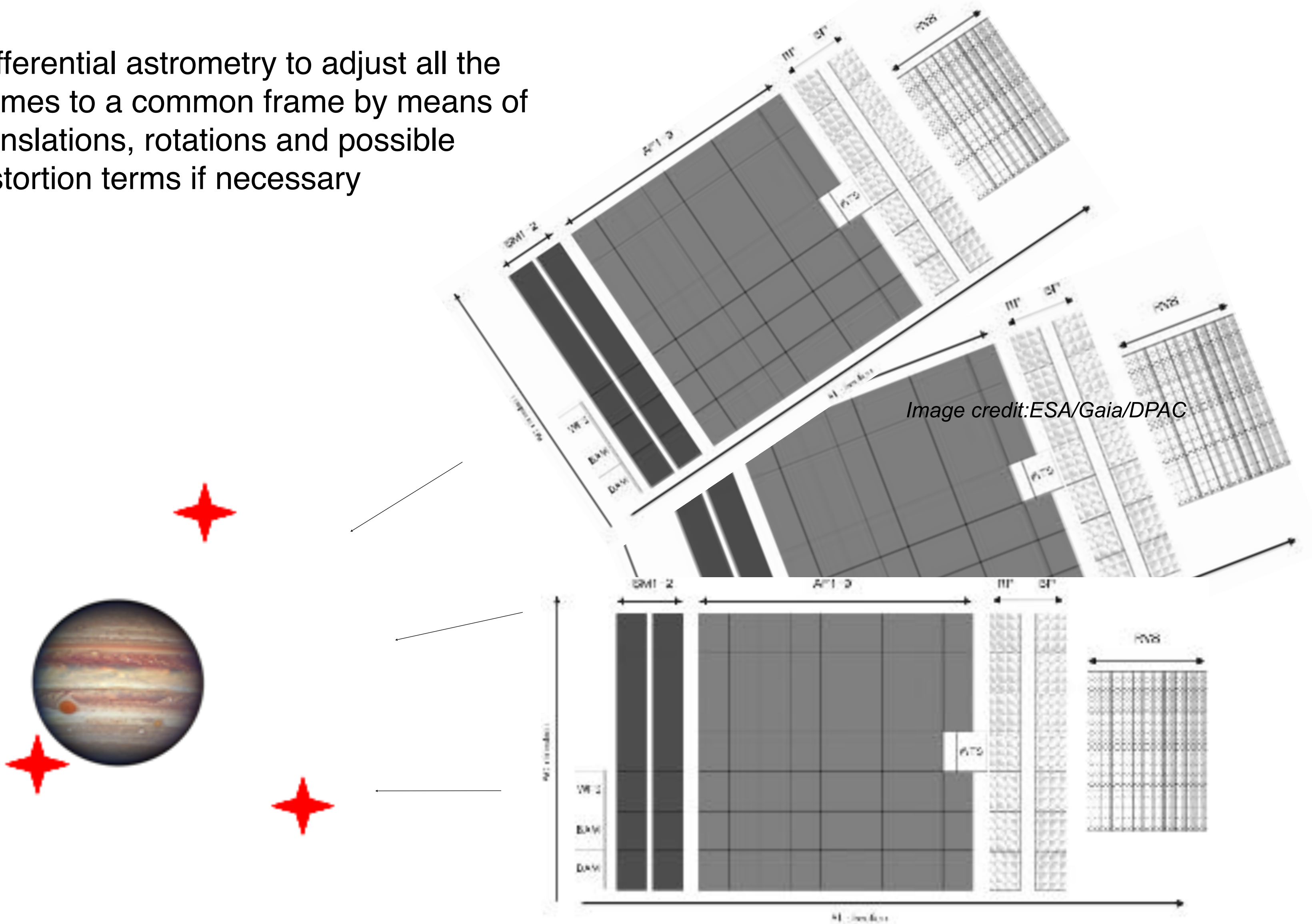

Image credit:ESA/Gaia/DPAC

Differential astrometric analysis of the star observations developed at INAF-OATo via the DPCT

Different scenes of stars (red points) around the Target star (blue point) as seen by Gaia on different transits. The top left panel also shows the positions of Jupiter during the Feb transits as large red points.

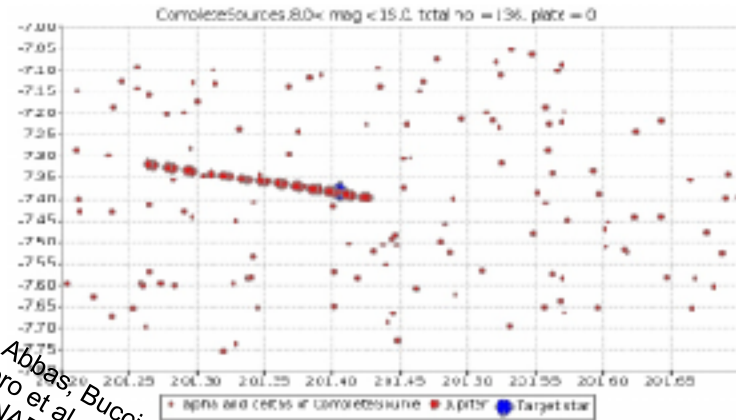

Figure: Stars seen in Jan

(From Abbas, Bucciarelli, Crosta, MGL, Busonero et al. 2017, Gaia TN, GAIA-C3-TN-INAF-UA-005-01)

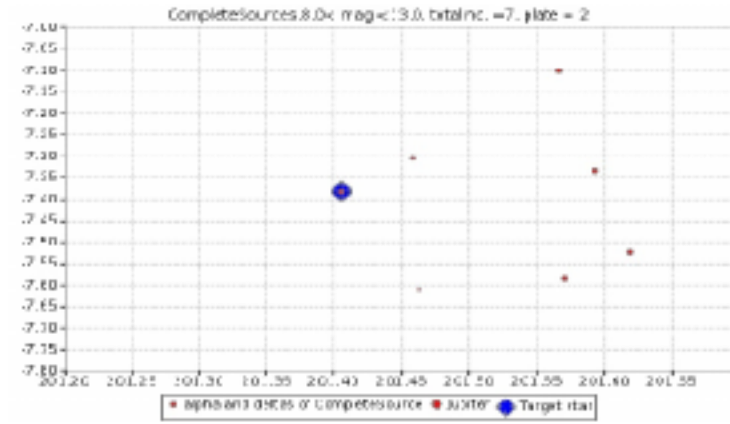

Figure: Stars seen on 2nd transit

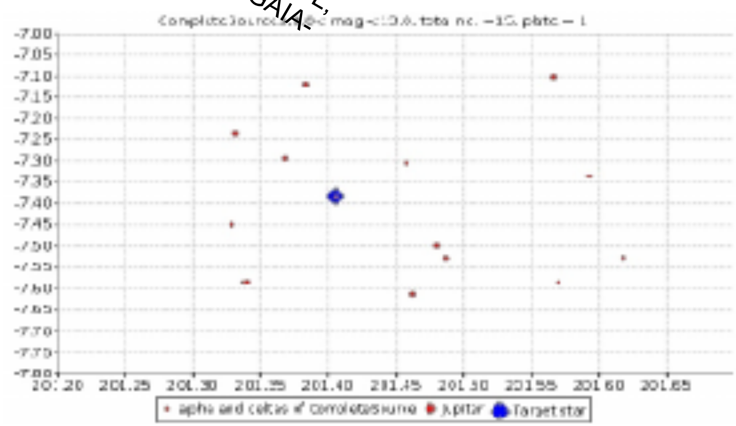

Figure: Stars seen on 1st transit

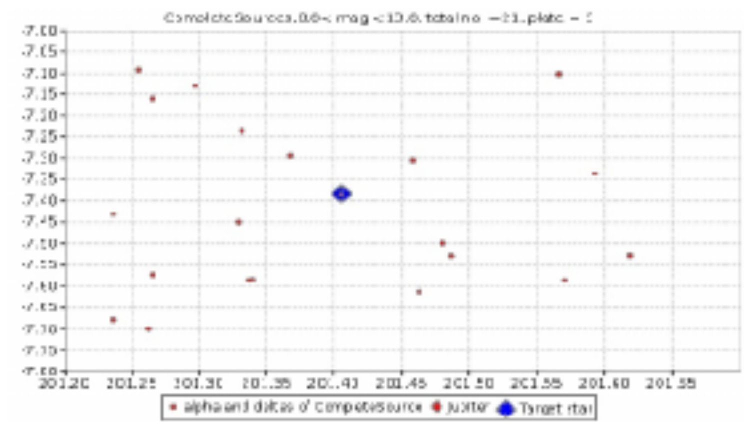

Figure: Stars seen on 3rd transit

Challenges of the scenario

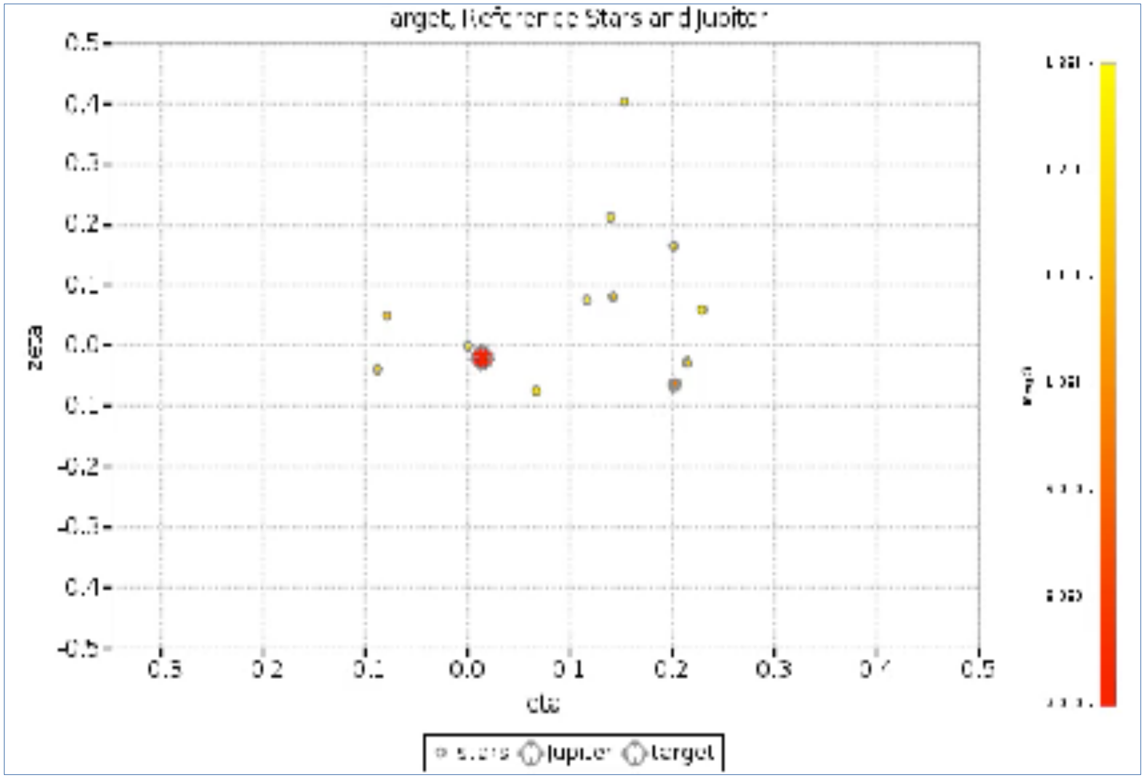

The star field (G<13 mag) as seen by Gaia (simulation) on a succession of transits (15 transits chosen around the time of closest approach by the target) along with the motion of Jupiter.

Challenges of the scenario

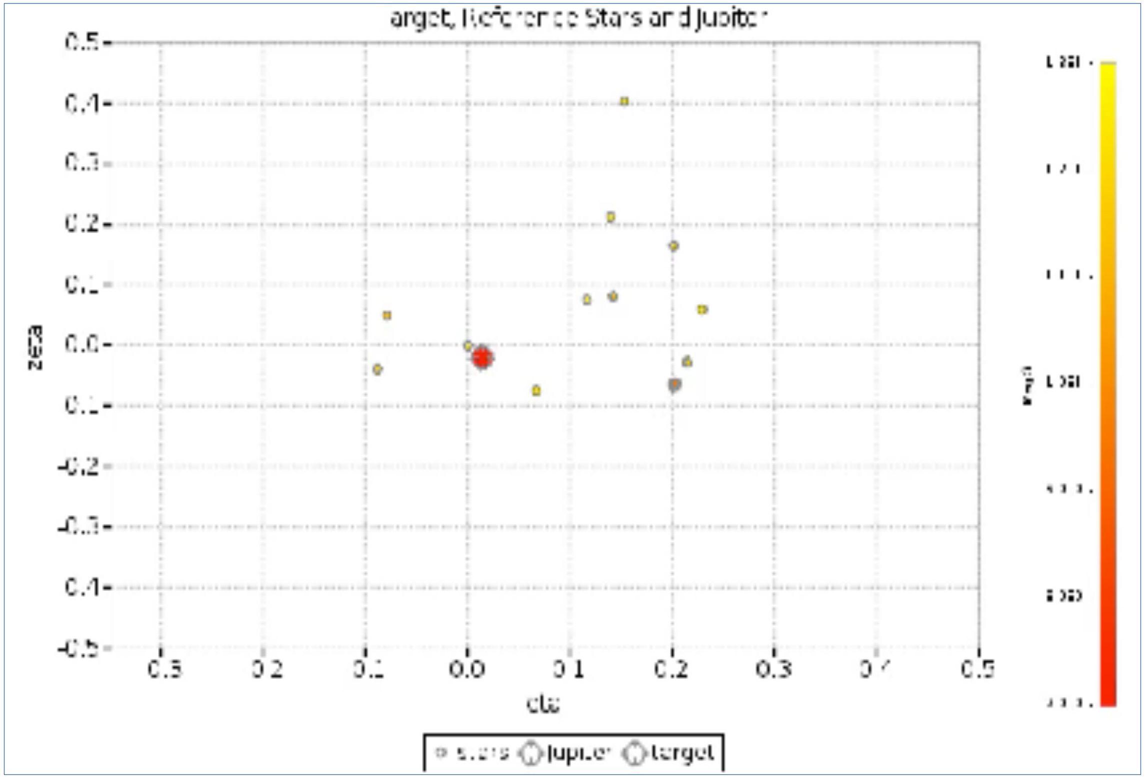

The star field (G<13 mag) as seen by Gaia (simulation) on a succession of transits (15 transits chosen around the time of closest approach by the target) along with the motion of Jupiter.

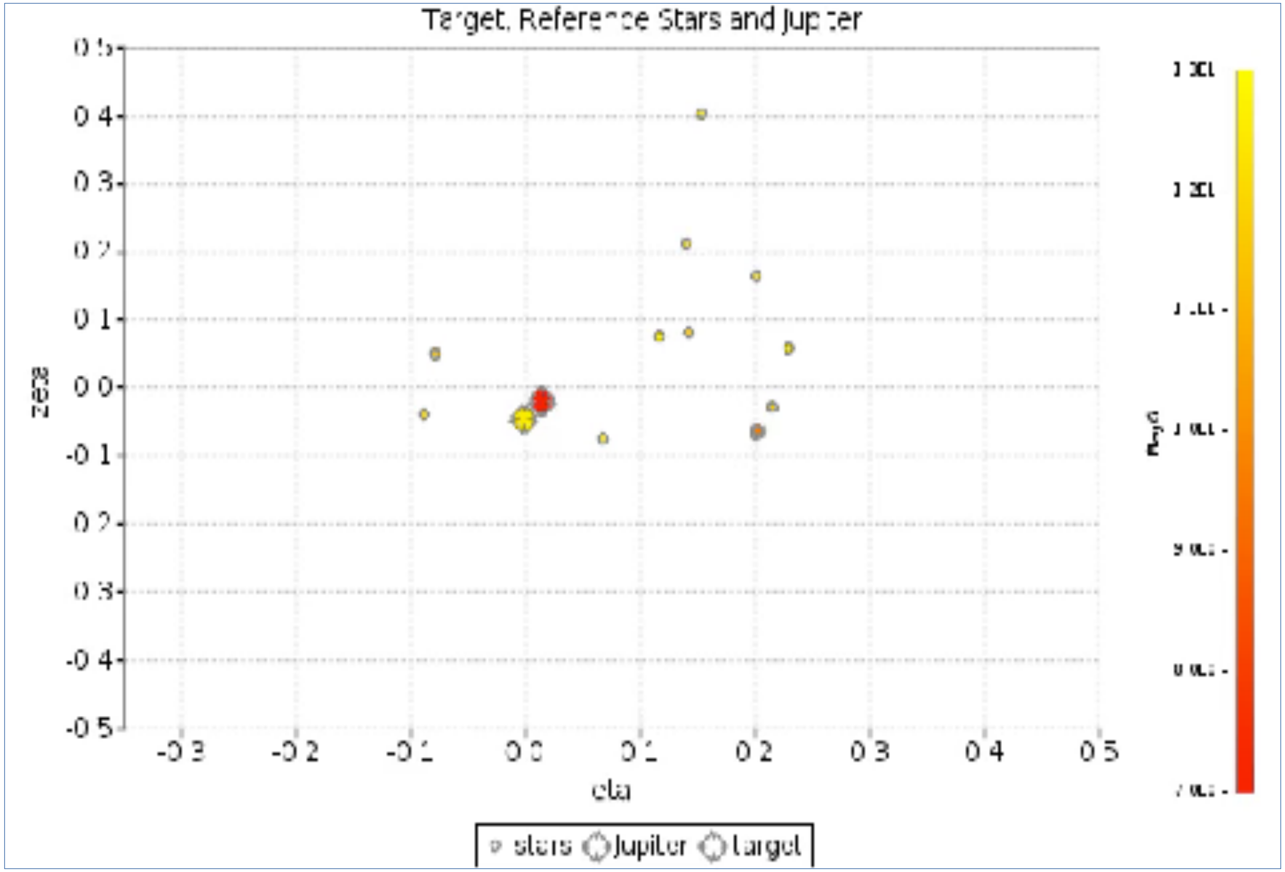

Simulation of the monopole deflection effect shown here enlarged by a factor of 50,000.

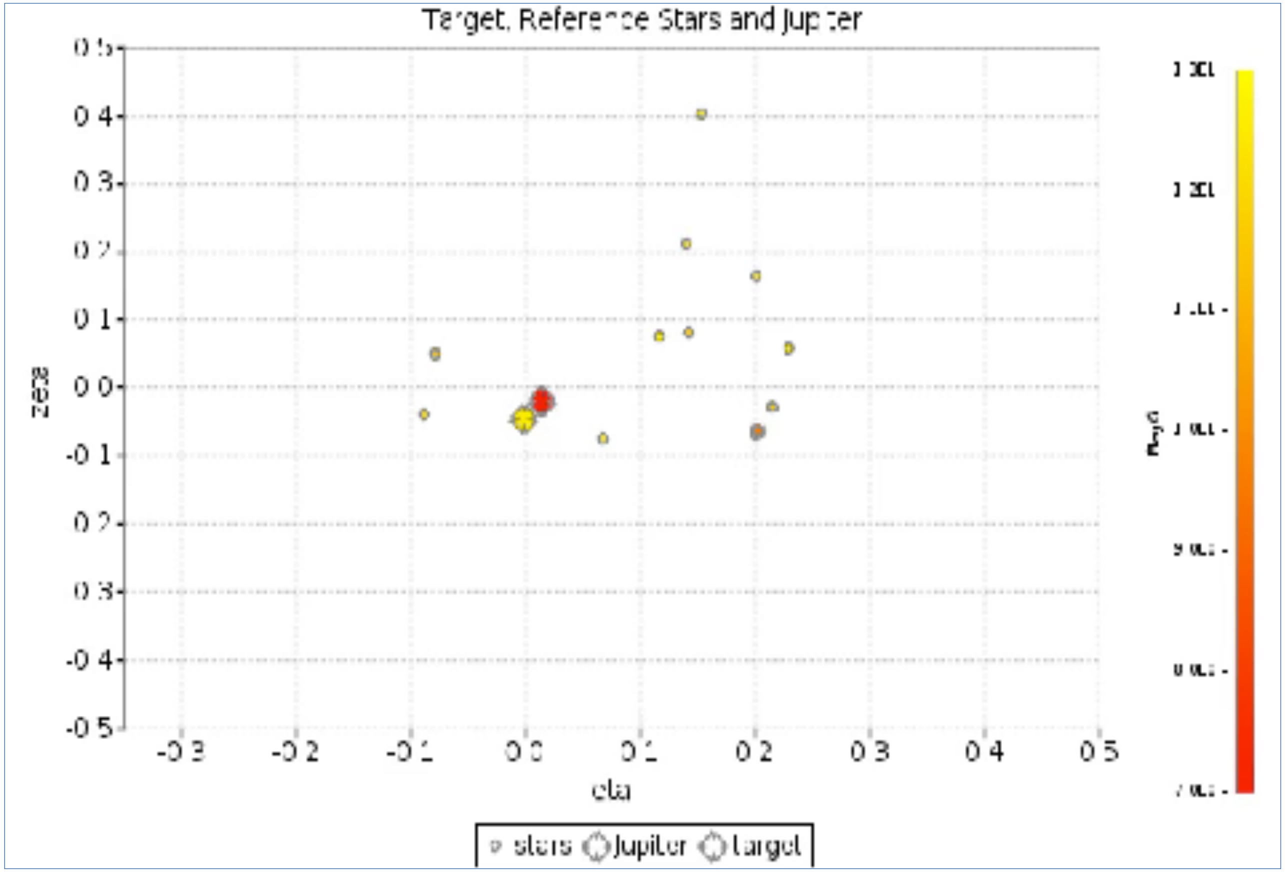

Simulation of the monopole deflection effect shown here enlarged by a factor of 50,000.

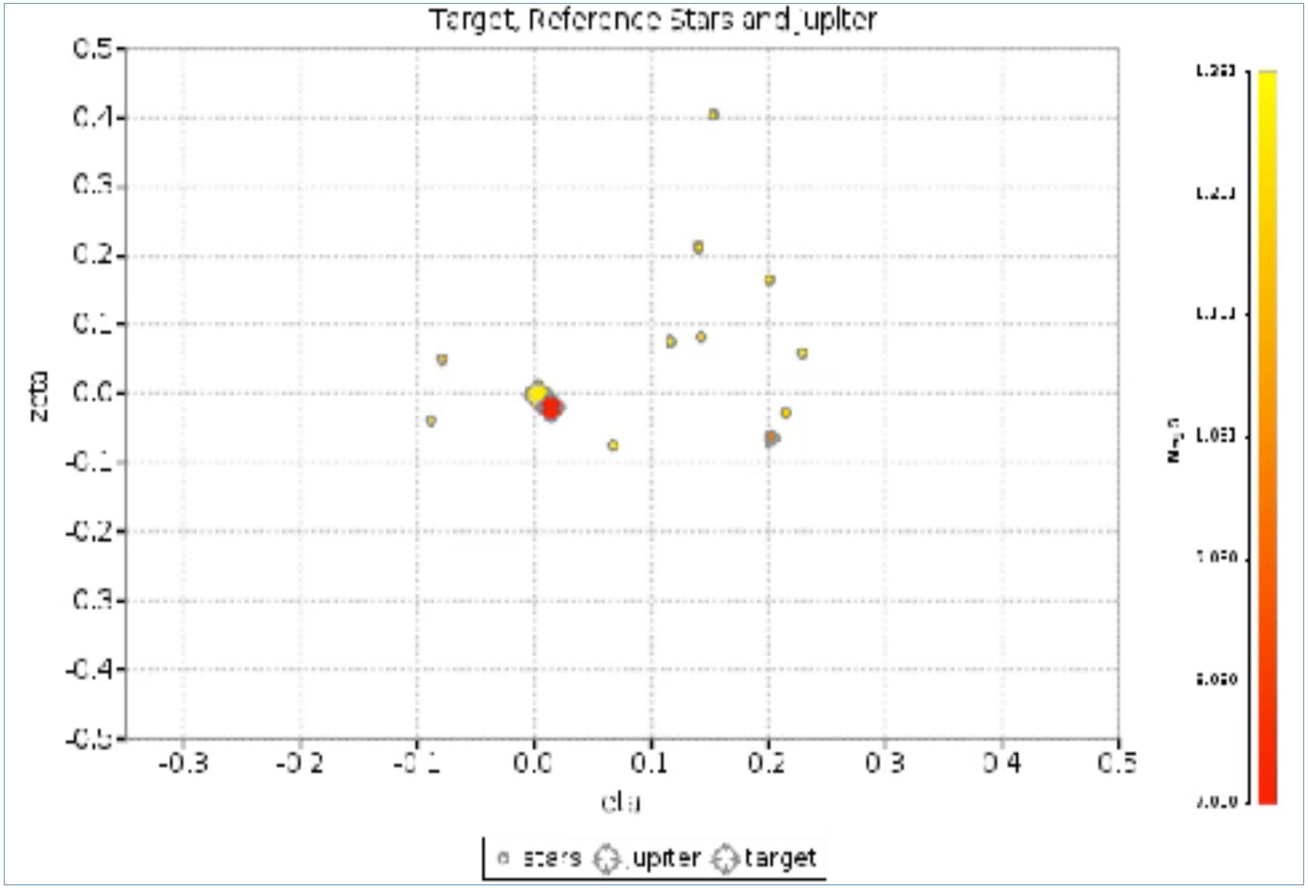

*Simulation of the quadrupole deflection effect shown here enlarged by a factor of 70*50,000.*

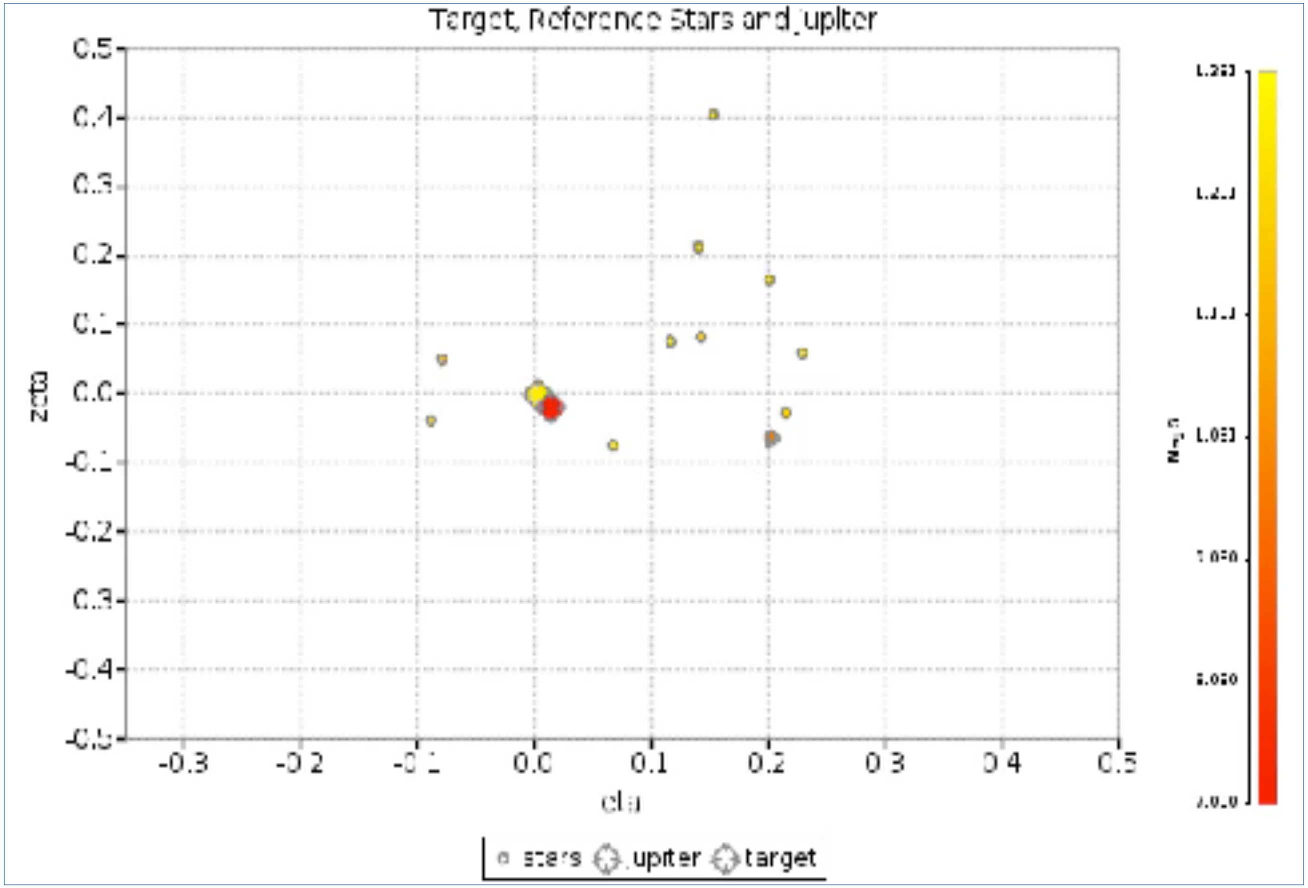

*Simulation of the quadrupole deflection effect shown here enlarged by a factor of 70*50,000.*

Deflection signal

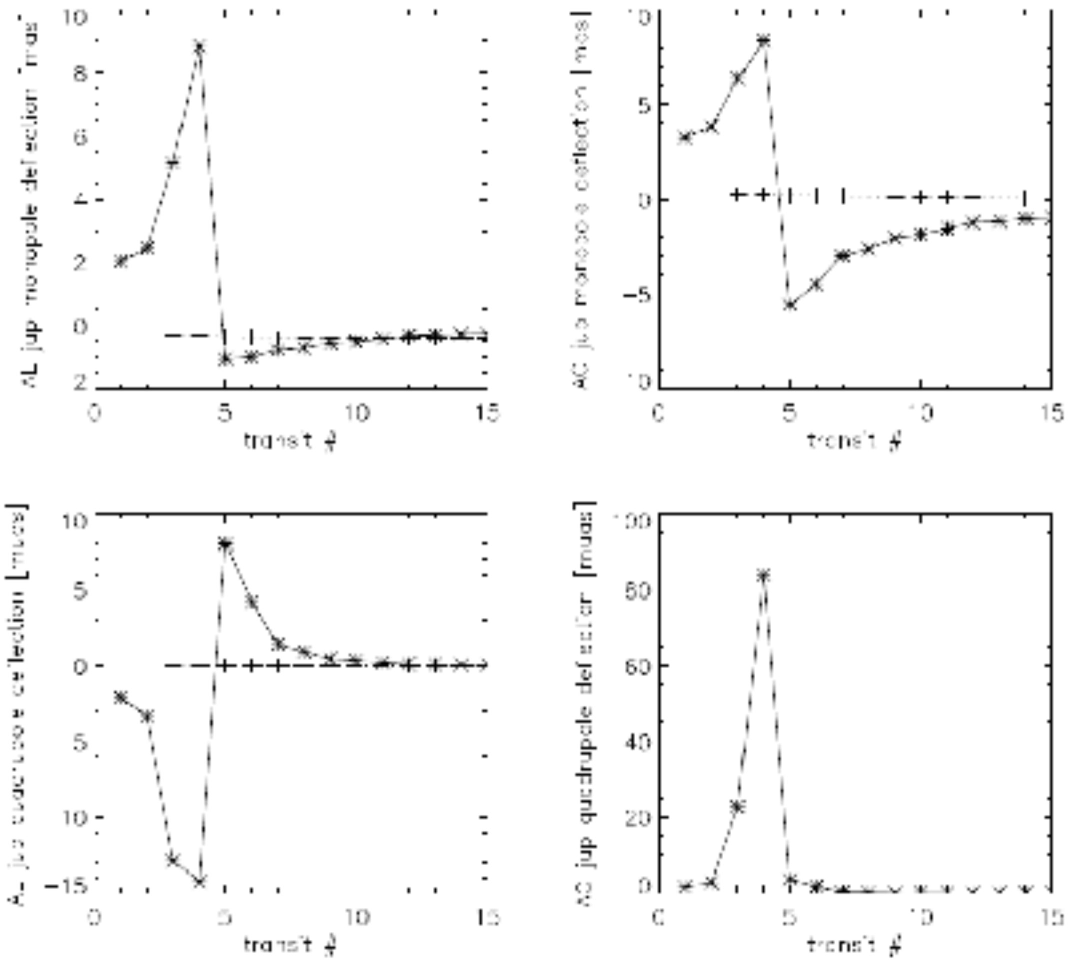

Upper panels show the simulated AL/AC monopole deflection signal and lower panels the quadrupole deflection signal.

Asterisks denote the target star and plus signs a randomly chosen reference star.

QDIFF: Systematic Effects

Physical Effects

- ***Gravitational deflection of light*** *due to Solar System Objects*
- ***Aberration*** *due to motion of Observer wrt barycenter of the Solar System*
- ***Effect due to the AL-AC motion of a star***
- ***Star's Proper Motion*** *leads to differential effects of several tens of micro-arcsec*

Instrumental Effects

- ***Time-dependent instrument model*** *describing the layout of the CCDs*
- ***physical geometry of each individual CCD*** *and its configuration in the FP assembly*
- *the* ***distortions and aberrations in the optical system***
- ***nominal values*** *of the focal length and basic angle*

QDIFF: Systematic Effects

Physical Effects

- ***Gravitational deflection of light*** *due to Solar System*
- ***Aberration*** *due to motion of Observer wrt barycenter c*

$$\delta\theta_{ab} = \frac{v}{c}\sin\theta\left[1 + \frac{1}{c^2}(1+\gamma)w(x_0) + \frac{1}{4}\frac{v^2}{c^2}\right] - \frac{1}{4}\frac{v^2}{c^2}\sin 2\theta + \frac{1}{12}\frac{v^3}{c^3}\sin 3\theta + O(c^{-4})$$

- ***Effect due to the AL-AC motion of a star***
- ***Star's Proper Motion*** *leads to differential effects of several tens of micro-arcsec*

Instrumental Effects

- ***Time-dependent instrument model*** *describing the layout of the CCDs*
- ***physical geometry of each individual CCD*** *and its configuration in the FP assembly*
- *the* ***distortions and aberrations in the optical system***
- ***nominal values*** *of the focal length and basic angle*

QDIFF: Systematic Effects

Physical Effects

- ***Gravitational deflection of light*** *due to Solar System Objects*
- ***Aberration*** *due to motion of Observer wrt barycenter of the Solar System*
- ***Effect due to the AL-AC motion of a star***
- ***Star's Proper Motion*** *leads to differential effects of several tens of micro-arcsec*

Instrumental Effects

- ***Time-dependent instrument model*** *describing the layout of the CCDs*
- ***physical geometry of each individual CCD*** *and its configuration in the FP assembly*
- *the* ***distortions and aberrations in the optical system***
- ***nominal values*** *of the focal length and basic angle*

QDIFF: Systematic Effects

Physical Effects

- ***Gravitational deflection of light*** *due to Solar System Objects*
- ***Aberration*** *due to motion of Observer wrt barycenter of the Solar System*
- ***Effect due to the AL-AC motion of a star***
- ***Star's Proper Motion*** *leads to differential effects of several* c

$$\eta(t_i) = \eta(t_S) + \frac{d\eta}{dt} * (t_i - t_S)$$

$$\zeta(t_i) = \zeta(t_S) + \frac{d\zeta}{dt} * (t_i - t_S)$$

Instrumental Effects

- ***Time-dependent instrument model*** *describing the layout of the CCDs*
- ***physical geometry of each individual CCD*** *and its configuration in the FP assembly*
- *the* ***distortions and aberrations in the optical system***
- ***nominal values*** *of the focal length and basic angle*

QDIFF: Systematic Effects

Physical Effects

- ***Gravitational deflection of light*** *due to Solar System Objects*
- ***Aberration*** *due to motion of Observer wrt barycenter of the Solar System*
- ***Effect due to the AL-AC motion of a star***
- ***Star's Proper Motion*** *leads to differential effects of several tens of micro-arcsec*

Instrumental Effects

- ***Time-dependent instrument model*** *describing the layout of the CCDs*
- ***physical geometry of each individual CCD*** *and its configuration in the FP assembly*
- *the* ***distortions and aberrations in the optical system***
- ***nominal values*** *of the focal length and basic angle*

QDIFF: Systematic Effects

Physical Effects

- ***Gravitational deflection of light*** *due to Solar System Objects*
- ***Aberration*** *due to motion of Observer wrt barycenter of the Solar System*
- ***Effect due to the AL-AC motion of a star***
- ***Star's Proper Motion*** *leads to differential effects of several tens of micro-arcsec*

$$\frac{d\eta}{dt} = -\omega_z + [\omega_x \cos\varphi + \omega_y \sin\varphi] \tan\zeta$$
$$\frac{d\zeta}{dt} = -\omega_x \sin\varphi + \omega_y \cos\varphi$$

Instrumental Effects

- ***Time-dependent instrument model*** *describing the layout of the CCDs*
- ***physical geometry of each individual CCD*** *and its configuration in the FP assembly*
- *the* ***distortions and aberrations in the optical system***
- ***nominal values*** *of the focal length and basic angle*

QDIFF: Systematic Effects

Physical Effects

- ***Gravitational deflection of light*** *due to Solar System Objects*
- ***Aberration*** *due to motion of Observer wrt barycenter of the Solar System*
- ***Effect due to the AL-AC motion of a star***
- ***Star's Proper Motion*** *leads to differential effects of several tens of micro-arcsec*

Instrumental Effects

- ***Time-dependent instrument model*** *describing the layout of the CCDs*
- ***physical geometry of each individual CCD*** *and its configuration in the FP assembly*
- *the* ***distortions and aberrations in the optical system***
- ***nominal values*** *of the focal length and basic angle*

QDIFF: Systematic Effects

Physical Effects

- ***Gravitational deflection of light*** *due to Solar System Objects*
- ***Aberration*** *due to motion of Observer wrt barycenter of the Solar System*
- ***Effect due to the AL-AC motion of a star***
- ***Star's Proper Motion*** *leads to differential effects of several tens of micro-arcsec*

Instrumental Effects

- ***Time-dependent instrument model*** *describing the layout of the CCDs*
- ***physical geometry of each individual CCD*** *and its configuration in the FP assembly*
- *the* ***distortions and aberrations in the optical system***
- ***nominal values*** *of the focal length and basic ang*

$$\eta_{fn}(\mu,t) \quad \eta^{0}_{n} + \sum_{r=0}^{2} \Delta\eta_{rfn} L^{*}_{r}\left(\frac{\mu \quad 13.5}{1966}\right)$$

QDIFF: Systematic Effects

Physical Effects

- ***Gravitational deflection of light*** *due to Solar System Objects*
- ***Aberration*** *due to motion of Observer wrt barycenter of the Solar System*
- ***Effect due to the AL-AC motion of a star***
- ***Star's Proper Motion*** *leads to differential effects of several tens of micro-arcsec*

Instrumental Effects

- ***Time-dependent instrument model*** *describing the layout of the CCDs*
- ***physical geometry of each individual CCD*** *and its configuration in the FP assembly*
- *the* ***distortions and aberrations in the optical system***
- ***nominal values*** *of the focal length and basic angle*

QDIFF: modeling

linear ‘plate model’

$$X'_{ij}(t_{it}) = X_{ij}(t_{ij}) + \sum_{r=0}^{2} \Delta\eta_{rfn} L_r^* \left(\frac{\rho - 13.5}{1966}\right)$$
$$+ (-\omega_{zv} + [\omega_{xv}\cos\varphi + \omega_{yv}\sin\varphi]\tan\zeta) * (t_{it} - t_{ij})$$
$$Y'_{ij}(t_{it}) = Y_{ij}(t_{ij}) + \sum_{r=0}^{2} \Delta\zeta_{rfn} L_r^* \left(\frac{\rho - 13.5}{1966}\right)$$
$$+ (-\omega_{xv}\sin\varphi + \omega_{yv}\cos\varphi) * (t_{it} - t_{ij})$$
$$\eta'_{0j}(t_{0t}) = a_i X'_{ij}(t_{it}) + b_i Y'_{ij}(t_{it}) + c_i - \mu_{\eta j}\Delta t_{ij}$$
$$\zeta'_{0j}(t_{0t}) = d_i X'_{ij}(t_{it}) + e_i Y'_{ij}(t_{it}) + g_i - \mu_{\zeta j}\Delta t_{ij}$$

Abbas, Bucciarelli et al. 2017

Parameters estimated using GaussFit (Jefferys et al. 1988): robust least squares estimator

Local cosmology with Gaia/galactic rotational curve

Milky Way (MW) as a product of a cosmological evolution at z=0

The thick disk and the local inner halo of Milky Way as chemo-dynamical lab for testing galactic models and compare **(Λ)CDM predictions/GR**

©P. Harding e H. Morrison

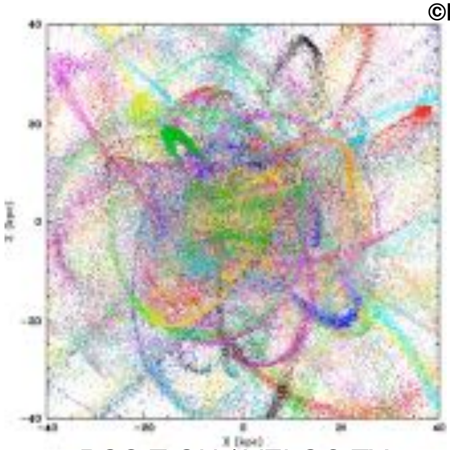

POSITION / VELOCITY

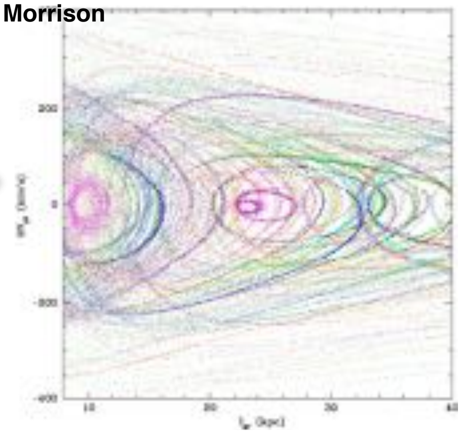

POSITION / POSITION

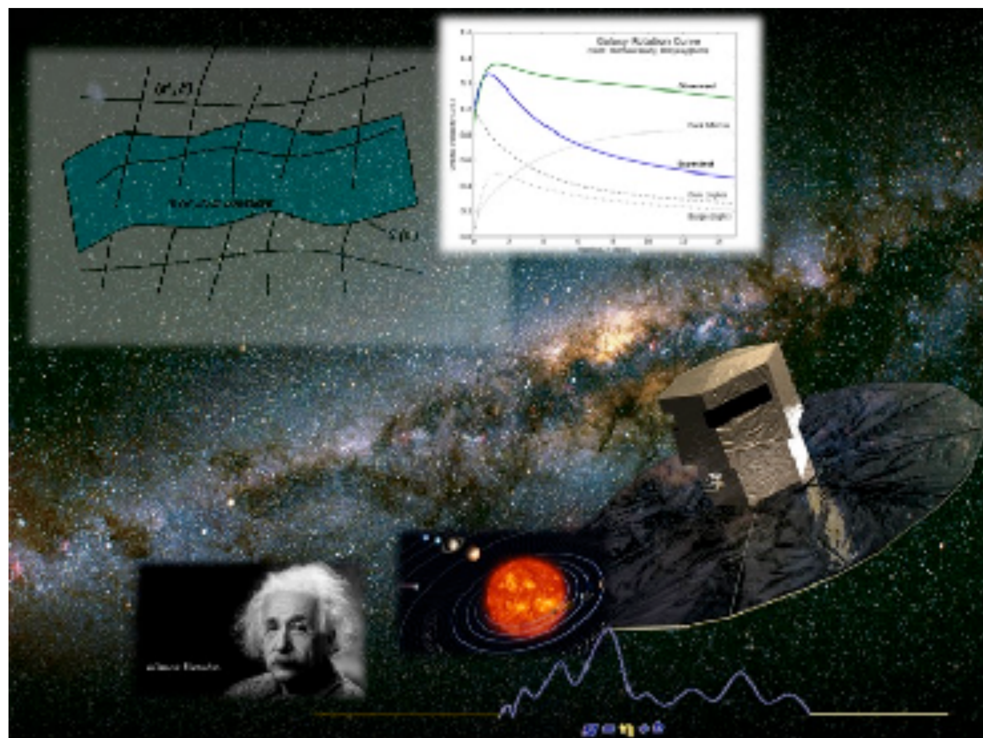

Gravitational Astrometry and relativistic Galactic models

PHD-INAF *M. Giammaria*

SV *M. Crosta*
co-SV *MGL Lattanzi*

✓Stressing the point

- In the most advanced simulations nowadays, GR is only partially considered:

“ Friedeman tells space how to curve and Newton tells mass how to move”
arXiv:1612.09309v2, Alan A. Coley, David L. Wiltshire

standards Lambda-CDM cosmology assumes an average FLRW evolution while growth in structure is treated by Newtonian N-body simulations

-The use of Gaia data must be parallel with the utilization of the most advanced cosmological simulations with baryonic matter (gas and stars) tracing its chemo-dynamics evolution at a high resolution level

- the position and velocity data comprising the output of the Gaia mission are fully GR compliant -> building **consistent observables**

➢ Once a relativistic model for the data reduction has been implemented, any subsequent scientific exploitation should be consistent with the precepts of the theory underlying such a model

-The GR picture of the MW is the only way to ensure a strong and coherent Local Cosmology laboratory against which the current formation and evolution model can be totally tested.

the failure of GR should be proved using the GR theory not the Newtonian one!

In general one assumes that:
velocity of stars in Galaxy is small: v/c<10^−3
gravity is weak in Galaxy (besides the centre)
then locally Newton approximation valid at each point!
But Galaxy is not a point source but an extended source..

a "toy model" for Galaxy disk:

exact stationary axially symmetric solutions of the 4-dim. Ein.eq. with co-rotating pressureless perfect fluid source

$$ds^2 = -(dt - N\, d\phi)^2 + r^2\, d\phi^2 + e^{\nu}(dr^2 + dz^2)$$

3-velocity distribution of the co-rotating dust as seen by an asymptotic observer at rest wrt to the center of the Galaxy (or the rotation axis)

$$V(r,z) = \frac{N(r,z)}{r}$$

$$N(r,z) = V_0(R - r_0) + \frac{V_0}{2}\sum_{\pm}\left(\sqrt{(z \pm r_0)^2 + r^2} - \sqrt{(z \pm R)^2 + r^2}\right)$$

$(V_0 \approx 200\ km/s \approx 7 * 10^{-4})$

$$V(r,0) = \frac{V_0}{r}\left(R - r_0 + \sqrt{r_0^2 + r^2} - \sqrt{R^2 + r^2}\right)$$

bulge radius r_0 is set to 1 kpc and R to 100 kpc.

Balasin and Grumiller (**BG**),
2008,Int.J.Mod.Phys.D17:475-488,2008

preliminary fit with the Gaia DR2 data

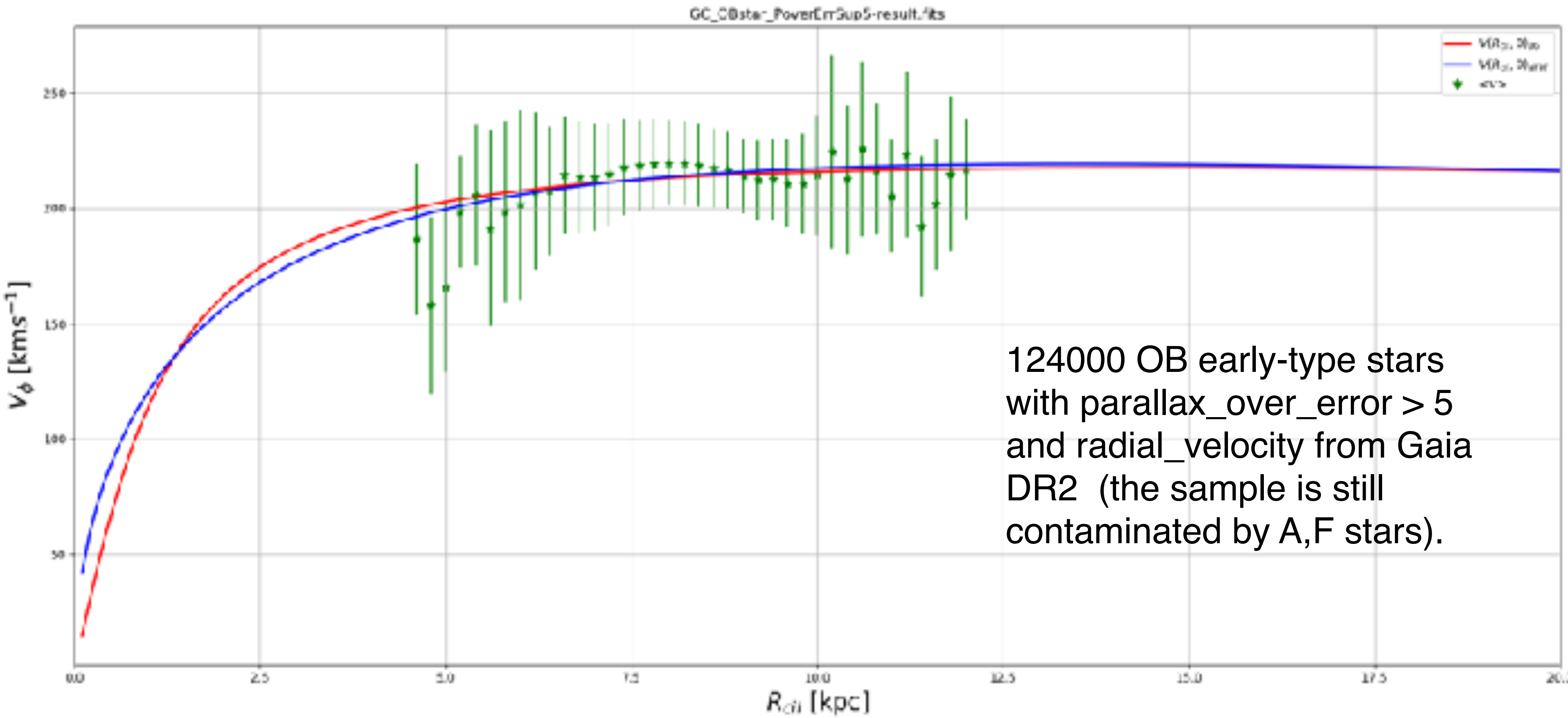

Green dots represent stellar average velocity in a shell of (r, r+ 0.2) kpc, error = velocity dispersion inside the corresponding shell.

- blu Navarro- Frenk_White profile -> virial radius about 180 kpc, velocity about 160 km/s, halo scale radius about 10 kpc

- red BG galactic “relativistic” curve -> “cylindrical “ internal radius z about 1kpc, external “viral “ radius about 135 kpc, V_rot from the Sun about 230 km/s

fits compatible with the data and same chi2

√Concluding remarks

The realization of the **relativistic celestial sphere** is an all-sky scientific validation of the absolute parallax and proper motions in Gaia. But reaching 10-20 μas accuracy on individual parallax and annual proper motions for bright stars (V<16) is also the largest GR experiment ever attempted from space

Lesson from Gaia: ***the power of the weak (non-linear) gravitational fields*** **both at Solar System/MW scales**

astrometry cannot be set apart from fundamental physics, high accuracy needs new refinement of the observable according to GR

To trace light trajectories back to the emitting stars requires an appropriate treatment of local gravity and a relativistic definition of the observable, according to the measurement protocol of GR.
Null geodesic should be as fundamental as the equation of stellar evolution!

GR weak field regime *is not* always equivalent to Newtonian regime..

➢ DR1 results and DR2 processing and validation are indicating that the Gaia mission can fulfill most of the science promised

At DR2 and after (<u>with external photometric and spectroscopic information</u>)

- Global (all-sky) GR tests from within the Solar System
- Non-Newtonian rotational curves
- Hypervelocity stars
- Local Cosmology:
  - Galactic Warp via new proper motions/distances of O-B stars
  - Thick Disk velocity-metallicity correlation at 8 kpc from Gal. Cen.
  - Structure in the inner halo (within 3-5 kpc around the Sun)

- DR1 results and DR2 processing and validation are indicating that the Gaia mission can fulfill most of the science promised

At DR2 and after (<u>with external photometric and spectroscopic information</u>)

- Global (all-sky) GR tests fro
- Non-Newtonian rotational cu
- Hypervelocity stars
- Local Cosmology:
  - Galactic Warp via new proper motions/distances of O-B stars
  - Thick Disk velocity-metallicity correlation at 8 kpc from Gal. Cen.
  - Structure in the inner halo (within 3-5 kpc around the Sun)

- DR1 results and DR2 processing and validation are indicating that the Gaia mission can fulfill most of the science promised

At DR2 and after (with external photometric and spectroscopic information)

- Global (all-sky) GR tests from within the Solar System
- Non-Newtonian rotational curves
- Hypervelocity stars
- Local Cosmology:
  - Galactic Warp via new proper motions/distances of O-B stars
  - Thick Disk velocity-metallicity correlation at 8 kpc from Gal. Cen.
  - Structure in the inner halo (within 3-5 kpc around the Sun)

➢ DR1 results and DR2 processing and validation are indicating that the Gaia mission can fulfill most of the science promised

At DR2 and after (with external photometric and spectroscopic information)

- Global (all-sky) GR tests from within the Solar System
- Non-Newtonian rotational curves
- Hypervelocity stars
- Local Cosmology:
  - Galactic Warp via new proper motions/distances of O-B stars E. Poggio et al., 2018, MNRAS, *Warped kinematics of the Milky Way revealed by Gaia*
  - Thick Disk velocity-metallicity correlation at 8 kpc from Gal. Cen.
  - Structure in the inner halo (within 3-5 kpc around the Sun)

➢ DR1 results and DR2 processing and validation are indicating that the Gaia mission can fulfill most of the science promised

At DR2 and after (with external photometric and spectroscopic information)

- Global (all-sky) GR tests from within the Solar System
- Non-Newtonian rotational curves
- Hypervelocity stars
- Local Cosmology:
  - Galactic Warp via new proper motions/distances of O-B stars
  - Thick Disk velocity-metallicity correlation at 8 kpc from Gal. Cen.
  - Structure in the inner halo (within 3-5 kpc around the Sun)

✓Beyond Gaia

<u>Gaia represents ONLY the 1-step</u>… increasing the level of the measurement precision requires to refine consistently the metric of the solar system, the solution for the null geodesic and so on..

➢**individual distances, space-phase stellar distributions can be achieved only from "in situ" investigations** i.e. from within the local universe

➢μas accuarcy is not enough to probe directly Mpc scale -> nanoarcsec regime and GWs!

➢ Gaia's astrometric released data fully compliant with the prescriptions of GR. The comparison, simulated data are not!

"***One day, our actual knowledge of the composition of the fixed stars sky, the apparent motion of the fixed stars, and the position of the spectral lines as a function of the distance will probably have come far enough for us to be able to decide empirically the question whether or not Λ vanishes"***

[Einstein, 1917, letter to de Sitter]